

Octet baryon and heavy meson interactions in chiral effective field theory

Bo-Lin Huang ^{*1}, Bo Wang ^{†2,3,4}, and Shi-Lin Zhu ^{‡5}

¹*School of Physical Science and Technology, Inner Mongolia University, Hohhot 010021, China*

²*College of Physics Science & Technology, Hebei University, Baoding 071002, China*

³*Hebei Key Laboratory of High-precision Computation and Application of Quantum Field Theory, Baoding, 071002, China*

⁴*Hebei Research Center of the Basic Discipline for Computational Physics, Baoding, 071002, China*

⁵*School of Physics and Center of High Energy Physics, Peking University, Beijing 100871, China*

February 2, 2024

Abstract

We calculate the effective potentials of the octet baryon and heavy meson systems using the chiral effective field theory up to the next-to-leading order. We consider the contact terms, one-pseudoscalar-meson and two-pseudoscalar-meson exchange contributions, facilitating a comprehensive analysis of the short-, mid-, and long-range interactions in these systems. The low energy constants (LECs) are correlated with those of the $\bar{N}N$ interaction using a quark-level Lagrangian approach. We also incorporate the decuplet baryon contributions in the loop diagrams. Our research provides new insights into several near-threshold charmed baryons [e.g., $\Lambda_c(2940)$, $\Xi_c(3055)$, and $\Omega_c(3188)$, etc.] around 3 GeV from the hadronic molecular perspective. We also identify several molecular states, designated as Ξ_c , within the mass range of 3100 – 3500 MeV. Further measurements of their resonance parameters and decay patterns in experiments will help to discriminate the conventional baryon and hadronic molecule explanations for these near-threshold states.

Keywords: Chiral effective field theory, Octet baryon and heavy meson interaction, Bound states

1 Introduction

Investigations of the baryon-meson interactions provide significant insights into quantum chromodynamics (QCD) at hadronic scales, forming a critical foundation for advancing hadron spectroscopy. The quark model, known for its efficacy in demystifying hadron spectra [1], faces substantial challenges in incorporating some near-threshold states such as $X(3872)$ [2] and $D_{s0}(2317)$ [3–5] within its theoretical framework [6–12]. These complications are similarly evident in charmed baryons, exemplified by $\Lambda_c(2940)$ and $\Xi_c(3055)$, which mirror the perplexities encountered with $X(3872)$ and $D_{s0}(2317)$.

The charmed baryon $\Lambda_c(2940)^+$ was first reported in 2007 by the BABAR Collaboration [13]. It was identified in the D^0p invariant mass spectrum. The $\Lambda_c(2940)^+$ was an isosinglet, evidenced by the absence of any signals in the D^+p final state. This discovery was later corroborated by the Belle experiment, which uncovered the decay mode of $\Lambda_c(2940)^+ \rightarrow \Sigma_c^{0,++}\pi^{+,-}$ [14]. Further advancements were made in 2017 when the LHCb Collaboration shed light on the quantum numbers J^P of $\Lambda_c(2940)^+$, suggesting $J^P = 3/2^-$ as the most likely spin-parity assignment [15].

There are two primary hypotheses on the internal structure of $\Lambda_c(2940)$: either a traditional charmed baryon or a D^*N molecular state. The latter proposition arises primarily due to the challenge of categorizing $\Lambda_c(2940)$ as a $2P$ state in the charmed baryon spectroscopy. Its mass

*blhuang@imu.edu.cn

†wangbo@hbu.edu.cn

‡zhushl@pku.edu.cn

falls short by approximately 60 – 100 MeV compared to the quark model predictions [16–19]. The molecular state hypothesis gained traction considering that $\Lambda_c(2940)$ is situated roughly 6 MeV below the $D^{*0}p$ threshold. The authors of ref. [20] analyzed its decay patterns and suggested $\Lambda_c(2940)$ as a $1/2^-$ molecular state. He *et al.* [21] examined the D^*N interaction via the one-boson-exchange model and endorsed the view of $\Lambda_c(2940)$ as a D^*N bound state with $I(J^P) = 0(1/2^+)$ or $0(3/2^-)$. Ortega *et al.* [22] delved into the D^*N molecular framework using the constituent quark model and deduced a binding solution in the isoscalar $J^P = 3/2^-$ channel. This molecular picture is further supported by the analyses of the strong and radiative decays of $\Lambda_c(2940)$ in refs. [23, 24]. Moreover, a QCD sum rule study [25] posits that $\Lambda_c(2940)$ does not manifest as a compact state. This perspective gains additional backing from recent calculations within the chiral quark model [26]. For a more in-depth exploration and diverse viewpoints on the nature and characteristics of $\Lambda_c(2940)$, one might consult the comprehensive reviews and related studies in refs. [27–49].

Baryons composed of one up or down quark, one strange quark, and one charmed quark are classified as Ξ_c baryons [1]. The landscape of charmed strange baryons has witnessed significant enrichment in recent years with the discovery of several highly excited states. Notably, the $\Xi_c(2980)$ and $\Xi_c(3080)$ baryons were first identified by the Belle Collaboration [50] and subsequently confirmed by the BABAR Collaboration [51]. Additionally, the BABAR Collaboration observed the $\Xi_c(3055)^+$ and $\Xi_c(3123)^+$ baryons [51]. However, only the $\Xi_c(3055)^+$ was later confirmed by the Belle Collaboration [52]. The Belle Collaboration [53] reported three charmed strange baryons. The $\Xi_c(3055)^0$ was first observed in the ΛD^0 decay mode, while the $\Xi_c(3055)^+$ and $\Xi_c(3080)^+$ were initially detected in the ΛD^+ decay mode. A notable aspect of these experiments is that the J^P (total angular momentum and parity) quantum numbers for most of the observed charmed baryons have not been determined.

Since its discovery, the $\Xi_c(3055)$ baryon has been the subject of extensive study. Liu *et al.* proposed that the $\Xi_c(3055)$ is a D -wave state based on their analysis of its strong decay [54]. Various studies have suggested different possibilities for the J^P of the $\Xi_c(3055)$, including $3/2^+$, $5/2^+$, and $7/2^+$, as detailed in refs. [18, 55–61]. Additionally, Ye *et al.* proposed in refs. [62, 63] that the $\Xi_c(3055)$ is not a P -wave excited Ξ_c baryon, but rather a $2S$ -wave state in the 3P_0 model. Contrary to these views, a molecular state description of the $\Xi_c(3055)$ was provided in ref. [64], suggesting its J^P as $1/2^-$. Given these diverse perspectives, it is clear that further research is essential to fully comprehend the nature of the $\Xi_c(3055)$ baryon.

The exploration of the octet baryon and heavy meson interactions is fundamental to resolving the mysteries associated with these charmed baryons. Moreover, a deep understanding of the octet baryon and heavy meson interactions is key to investigating the D -mesic nuclei [65, 66] as well as the characteristics of charmed mesons in nuclear environments [67, 68]. An alternative approach, the meson-exchange model [69], has been effectively utilized by the Jülich group [70–72] for the development of the DN and D^*N interaction framework.

The conceptual focus of modern nuclear force theory has shifted from the boson-exchange model to an approach more steeped in the foundational work of Weinberg [73, 74] and mainly shaped within the framework of effective field theory. Particularly, the chiral effective field theory has been widely and effectively utilized to examine the nucleon-nucleon (NN) interaction with significant success [75–80]. This theory has also shown considerable promise in the investigation of systems incorporating heavy flavors, as exemplified in various studies [81–90] (see ref. [12] for a recent review). The utility of the approach becomes apparent in its diverse application: projecting BB^* and B^*B^* bound states [83], deciphering the newly discovered pentaquarks [85], and extrapolating the $\Sigma_c N$ potential from the lattice QCD data to the physical pion mass [86] being some prominent examples.

In ref. [91], we examined the $D^{(*)}N$ interactions through chiral effective field theory. We extend our earlier research in this work. The findings from refs. [92–102] suggest that employing the SU(3) framework for such calculations yields plausible predictions. This current study aims to further explore the interactions between octet baryons and heavy mesons up to next-to-leading order within the chiral effective field theory. Our approach is comprehensive, incorporating the long-, mid-, and short-range interactions. Additionally, we include the contributions of the decuplet baryons, considering them as intermediate states in the loops. Utilizing chiral effective field theory, we not only calculate the effective potentials between the octet baryons and heavy mesons but also investigate the possible bound states.

This paper is structured as follows. Section 2 introduces the chiral Lagrangians. Section 3 covers Feynman diagrams and expressions of the effective potentials. Section 4 presents and

discusses our findings. The final section provides a brief summary. The Appendix includes the parameters for the potentials.

2 Chiral Lagrangian

Our calculation of the octet baryon and heavy meson interaction is based on the SU(3) effective chiral Lagrangian in the heavy hadron formulation,

$$\mathcal{L}_{\text{eff}} = \mathcal{L}_{B\phi} + \mathcal{L}_{B\phi T} + \mathcal{L}_{H\phi} + \mathcal{L}_{BH}. \quad (1)$$

The traceless hermitian 3×3 matrices B and ϕ include the octet baryon fields (N, Λ, Σ, Ξ) and the light pseudoscalar Goldstone boson fields ($\phi = \pi, K, \bar{K}, \eta$), respectively. The T represents the decuplet baryon fields ($\Delta, \Sigma^*, \Xi^*, \Omega$). The H is the superfield for the charmed mesons. The lowest-order SU(3) chiral Lagrangian for the octet baryon and light meson interaction take the form [103]

$$\mathcal{L}_{B\phi}^{(1)} = \text{tr}(i\bar{B}[v \cdot D, B]) + 2D\text{tr}(\bar{B}S_\mu\{u^\mu, B\}) + 2F\text{tr}(\bar{B}S_\mu[u^\mu, B]), \quad (2)$$

where $\text{tr}(\dots)$ represents the trace in flavor space, $v_\mu = (1, 0, 0, 0)$ is the heavy meson velocity, D_μ denotes the covariant derivative

$$[D_\mu, B] = \partial_\mu B + [\Gamma_\mu, B], \quad (3)$$

and S_μ is the covariant spin operator. In practice one works with $\vec{\sigma}$ (the Pauli spin matrices)

$$S^\mu = (0, \frac{\vec{\sigma}}{2}). \quad (4)$$

The chiral connection $\Gamma^\mu = [\xi^\dagger, \partial^\mu \xi]/2$ and the axial vector quantity $u^\mu = i\{\xi^\dagger, \partial^\mu \xi\}/2$ contain an even and odd number of meson fields, respectively. The SU(3) matrix $U = \xi^2 = \exp(i\phi/f)$ collects the light pseudoscalar Goldstone boson fields. The parameter f is the pseudoscalar decay constant in the chiral limit. The axial vector coupling constants D and F can be determined by fitting the semi-leptonic decays of the octet baryons [104]. The lowest-order SU(3) chiral Lagrangian involving the decuplet baryon takes the form [105]

$$\mathcal{L}_{B\phi T}^{(1)} = -\bar{T}^\mu(iv \cdot D - \delta_B)T_\mu + \mathcal{C}(\bar{T}^\mu u_\mu B + \bar{B}u_\mu T^\mu) + 2\mathcal{H}\bar{T}^\mu S \cdot uT_\mu, \quad (5)$$

where δ_B denotes the mass difference between the decuplet and octet baryon in the chiral limit. The chiral covariant derivative with the decuplet baryon field reads

$$iD_\mu T_{abc}^\nu = i\partial_\mu T_{abc}^\nu + (\Gamma_\mu)_a^d T_{dbc}^\nu + (\Gamma_\mu)_b^d T_{adc}^\nu + (\Gamma_\mu)_c^d T_{abd}^\nu, \quad (6)$$

with

$$T_{abc} = \begin{pmatrix} \Delta^{++} & \frac{\Delta^+}{\sqrt{3}} & \frac{\Sigma^{*+}}{\sqrt{3}} \\ \frac{\Delta^+}{\sqrt{3}} & \frac{\Delta^0}{\sqrt{3}} & \frac{\Sigma^{*0}}{\sqrt{6}} \\ \frac{\Sigma^{*+}}{\sqrt{3}} & \frac{\Sigma^{*0}}{\sqrt{6}} & \frac{\Xi^{*0}}{\sqrt{3}} \end{pmatrix} \begin{pmatrix} \frac{\Delta^+}{\sqrt{3}} & \frac{\Delta^0}{\sqrt{3}} & \frac{\Sigma^{*0}}{\sqrt{6}} \\ \frac{\Delta^0}{\sqrt{3}} & \Delta^- & \frac{\Sigma^{*-}}{\sqrt{3}} \\ \frac{\Sigma^{*0}}{\sqrt{6}} & \frac{\Sigma^{*-}}{\sqrt{3}} & \frac{\Xi^{*-}}{\sqrt{3}} \end{pmatrix} \begin{pmatrix} \frac{\Sigma^{*+}}{\sqrt{3}} & \frac{\Sigma^{*0}}{\sqrt{6}} & \frac{\Xi^{*0}}{\sqrt{3}} \\ \frac{\Sigma^{*0}}{\sqrt{6}} & \frac{\Sigma^{*-}}{\sqrt{3}} & \frac{\Xi^{*-}}{\sqrt{3}} \\ \frac{\Xi^{*0}}{\sqrt{3}} & \frac{\Xi^{*-}}{\sqrt{3}} & \Omega^- \end{pmatrix}. \quad (7)$$

In this representation, one can assign any particular permutation of indices a, b, c to denote the row, column, and sub-matrix. The decuplet remains completely symmetric after rearranging the flavor indices.

The lowest-order chiral Lagrangian for the heavy mesons reads [106, 107]

$$\mathcal{L}_{H\phi}^{(1)} = -\langle (iv \cdot \partial H)\bar{H} \rangle + \langle H(iv \cdot \Gamma)\bar{H} \rangle - \frac{1}{8}\delta_D \langle H\sigma^{\mu\nu}\bar{H}\sigma_{\mu\nu} \rangle + g \langle H u_\mu \gamma^\mu \gamma_5 \bar{H} \rangle, \quad (8)$$

where $\langle \dots \rangle$ represents the trace in spinor space and δ_D denotes the mass difference between the heavy pseudoscalar and vector meson. The doublet of the ground state heavy mesons reads

$$H = \frac{1+\not{v}}{2}(P_\mu^* \gamma^\mu + iP\gamma_5), \quad \bar{H} = \gamma^0 H^\dagger \gamma^0 = (P_\mu^{\dagger*} \gamma^\mu + iP^\dagger \gamma_5) \frac{1+\not{v}}{2}, \quad (9)$$

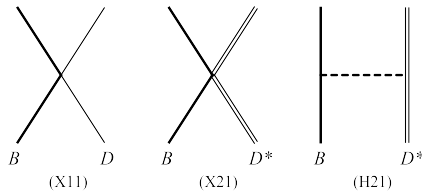


Figure 1: The leading order Feynman diagrams $\mathcal{O}(\epsilon^0)$ in the calculation of the octet baryon (B) and the heavy meson (D/D^*) effective potentials. The thick, thin, double-thin, and dashed lines denote the B , D , D^* , and ϕ fields, respectively.

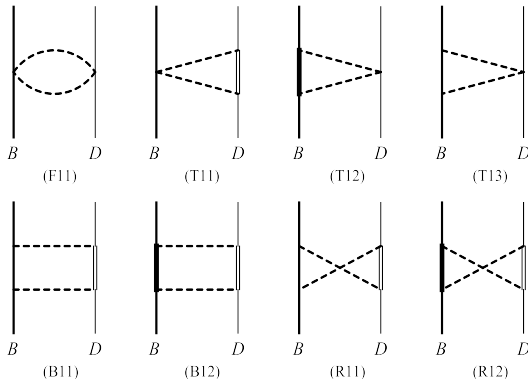


Figure 2: The two-pseudoscalar-meson-exchange diagrams for the BD system at $\mathcal{O}(\epsilon^2)$. These diagrams are categorized into the football diagram (F11), triangle diagrams (T11,T12,T13), box diagrams (B11,B12), and crossed box diagrams (R11,R12). The decuplet fields are represented by heavy-thick lines within the loops. The notations for other elements remain consistent with those presented in Fig. 1.

$$P = (D^0, D^+, D_s^+), \quad P_\mu^* = (D^{0*}, D^{+*}, D_s^{+*})_\mu. \quad (10)$$

At last, we construct the leading order contact Lagrangian to describe the short distance interaction between the octet baryon and heavy meson,

$$\begin{aligned} \mathcal{L}_{BH}^{(0)} = & D_a \text{tr}(\bar{B}B) \langle H\bar{H} \rangle + D_b \text{tr}(\bar{B}\gamma_\mu\gamma_5 B) \langle H\gamma^\mu\gamma_5\bar{H} \rangle \\ & + E_a \text{tr}(\bar{B}\lambda_a B) \langle H\lambda_a\bar{H} \rangle + E_b \text{tr}(\bar{B}\gamma_\mu\gamma_5\lambda_a B) \langle H\gamma^\mu\gamma_5\lambda_a\bar{H} \rangle, \end{aligned} \quad (11)$$

where D_a and D_b are two low energy constants that contribute to the central potential and the spin-spin interaction, respectively. On the other hand, E_a and E_b are associated with the isospin-isospin interaction, influencing the central potential and spin-spin interaction, respectively. With the quark model, we can determine their values using the nucleon-antinucleon interaction as inputs, as done in the Appendix of ref. [91]. The λ_a represents the conventional Gell-Mann matrix.

3 Expressions of the effective potentials

In the context of heavy hadron chiral perturbation theory, the scattering amplitudes for the BD and BD^* systems can be systematically expanded in a series. These expansions are based on small dimensionless parameters, denoted as $\epsilon = \{q/\Lambda_\chi, m_\phi/\Lambda_\chi, \delta/\Lambda_\chi\}$. Here, $\Lambda_\chi \simeq 1 \text{ GeV}$ represents the scale of chiral symmetry breaking. The parameter q refers to the momentum of Goldstone bosons or the residual momentum of heavy hadrons, m_ϕ indicates the masses of the light pseudoscalar mesons, and δ signifies the mass gap between the decuplet and octet baryons or between the heavy pseudoscalar and vector mesons. This power counting scheme is often denoted as the small scale expansion (SSE).

We present the explicit expressions of the effective potentials for the BD and BD^* systems at $\mathcal{O}(\epsilon^0)$. The corresponding Feynman diagrams are shown in Fig. 1, which contain the contact and one-pseudoscalar-meson exchange diagrams. The one-pseudoscalar-meson exchange diagram for

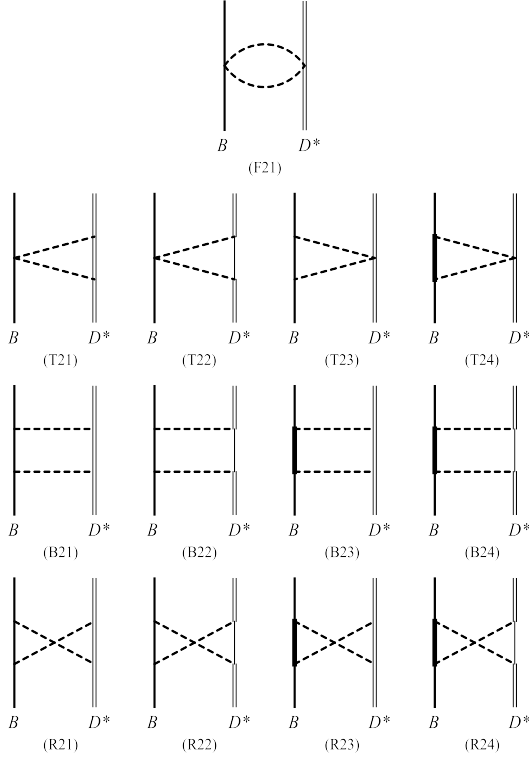


Figure 3: The two-pseudoscalar-meson-exchange diagrams for the BD^* system at $\mathcal{O}(\epsilon^2)$. The notations remain consistent with those depicted in Fig. 2.

the BD system vanishes because the three pseudoscalar meson vertex is forbidden. Then, the potentials read

$$\mathcal{V}_{BD}^{(X11)} = D_a + \alpha^{(X11)} E_a, \quad (12)$$

$$\mathcal{V}_{BD^*}^{(X21)} = D_a + D_b + \alpha^{(X21)} (E_a + E_b \boldsymbol{\sigma} \cdot \mathbf{T}), \quad (13)$$

$$\mathcal{V}_{BD^*}^{(H21)} = \alpha_\pi^{(H21)} \frac{g}{f_\pi^2} \frac{(\boldsymbol{\sigma} \cdot \mathbf{q})(\mathbf{T} \cdot \mathbf{q})}{\mathbf{q}^2 + m_\pi^2} + \alpha_\eta^{(H21)} \frac{g}{f_\eta^2} \frac{(\boldsymbol{\sigma} \cdot \mathbf{q})(\mathbf{T} \cdot \mathbf{q})}{\mathbf{q}^2 + m_\eta^2}, \quad (14)$$

where the parameters $\alpha^{(X11)}$, $\alpha^{(X21)}$, $\alpha_\pi^{(H21)}$, and $\alpha_\eta^{(H21)}$, which incorporate crucial isospin factors, are detailed in the Appendix. The operators $\boldsymbol{\sigma}$ and \mathbf{T} are connected to the spin operators of the spin- $\frac{1}{2}$ baryon and spin-1 meson, being represented as $(\frac{1}{2}\boldsymbol{\sigma})$ and $(-\mathbf{T})$ respectively. This relationship is elaborated in detail in ref. [85]. The Breit approximation formula,

$$\mathcal{V}(\mathbf{q}) = -\frac{\mathcal{M}(\mathbf{q})}{\sqrt{2M_1 2M_2 2M_3 2M_4}} \quad (15)$$

is employed to establish a connection between the scattering amplitude $\mathcal{M}(\mathbf{q})$ and the effective potential $\mathcal{V}(\mathbf{q})$ in momentum space, where $M_{1,\dots,4}$ are the masses of the scattering particles.

The two-pseudoscalar-meson-exchange diagrams for the BD system at order $\mathcal{O}(\epsilon^2)$ are shown in Fig. 2. The effective potentials from these diagrams read

$$\mathcal{V}_{BD}^{(F11)} = \alpha_{\pi\pi}^{(F11)} \frac{1}{f_\pi^4} J_{22}^F(m_\pi, m_\pi) + \alpha_{KK}^{(F11)} \frac{1}{f_K^4} J_{22}^F(m_K, m_K), \quad (16)$$

$$\mathcal{V}_{BD}^{(T11)} = \left\{ \frac{\alpha_{\pi\pi}^{(T11)}}{f_\pi^4}, \frac{\alpha_{KK}^{(T11)}}{f_K^4} \right\} g^2 \left[(d-1)J_{34}^T - (J_{24}^T + J_{33}^T) \mathbf{q}^2 \right] \{ (m_\pi, m_\pi, -\delta_D), (m_K, m_K, -\delta_D) \}, \quad (17)$$

$$\mathcal{V}_{BD}^{(T12)} = \left\{ \frac{\alpha_{\pi\pi}^{(T12)}}{f_\pi^4}, \frac{\alpha_{KK}^{(T12)}}{f_K^4} \right\} \mathcal{C}^2 \left[(2-d)J_{34}^T - \frac{2-d}{d-1} (J_{24}^T + J_{33}^T) \mathbf{q}^2 \right] \{ (m_\pi, m_\pi, -\delta_B), (m_K, m_K, -\delta_B) \}, \quad (18)$$

$$\mathcal{V}_{BD}^{(T13)} = \left\{ \frac{\alpha_{\pi\pi}^{(T13)}}{f_\pi^4}, \frac{\alpha_{KK}^{(T13)}}{f_K^4} \right\} \left[(d-1)J_{34}^T - (J_{24}^T + J_{33}^T) \mathbf{q}^2 \right] \{ (m_\pi, m_\pi), (m_K, m_K) \}, \quad (19)$$

$$\begin{aligned} \mathcal{V}_{BD}^{(B11)} = & \left\{ \frac{\alpha_{\pi\pi}^{(B11)}}{f_\pi^4}, \frac{\alpha_{KK}^{(B11)}}{f_K^4}, \frac{\alpha_{\eta\eta}^{(B11)}}{f_\eta^4}, \frac{\alpha_{\pi\eta}^{(B11)}}{f_\pi^2 f_\eta^2}, \frac{\alpha_{\eta\pi}^{(B11)}}{f_\eta^2 f_\pi^2} \right\} g^2 \left\{ (d^2-1)J_{41}^B - [J_{21}^B + 2(d+1)(J_{31}^B + J_{42}^B)] \mathbf{q}^2 \right. \\ & \left. + (J_{22}^B + 2J_{32}^B + J_{43}^B) \mathbf{q}^4 \right\} \{ (m_\pi, m_\pi, -\delta_D), (m_K, m_K, -\delta_D), (m_\eta, m_\eta, -\delta_D), \\ & (m_\pi, m_\eta, -\delta_D), (m_\eta, m_\pi, -\delta_D) \}, \end{aligned} \quad (20)$$

$$\begin{aligned} \mathcal{V}_{BD}^{(B12)} = & \left\{ \frac{\alpha_{\pi\pi}^{(B12)}}{f_\pi^4}, \frac{\alpha_{KK}^{(B12)}}{f_K^4}, \frac{\alpha_{\eta\eta}^{(B12)}}{f_\eta^4}, \frac{\alpha_{\pi\eta}^{(B12)}}{f_\pi^2 f_\eta^2}, \frac{\alpha_{\eta\pi}^{(B12)}}{f_\eta^2 f_\pi^2} \right\} \mathcal{C}^2 g^2 \frac{d-2}{d-1} \left\{ (J_{22}^B + 2J_{32}^B + J_{43}^B) \mathbf{q}^4 + (d^2-1)J_{41}^B \right. \\ & \left. - [J_{21}^B + 2(d+1)(J_{31}^B + J_{42}^B)] \mathbf{q}^2 \right\} \{ (m_\pi, m_\pi, -\delta_B, -\delta_D), (m_K, m_K, -\delta_B, -\delta_D), \\ & (m_\eta, m_\eta, -\delta_B, -\delta_D), (m_\pi, m_\eta, -\delta_B, -\delta_D), (m_\eta, m_\pi, -\delta_B, -\delta_D) \}, \end{aligned} \quad (21)$$

$$\mathcal{V}_{BD}^{(R11)} = \mathcal{V}_{BD}^{(B11)} \Big|_{J_{ij}^B \rightarrow J_{ij}^R, \alpha_{**}^{(B11)} \rightarrow \alpha_{**}^{(R11)}}, \quad (22)$$

$$\mathcal{V}_{BD}^{(R12)} = \mathcal{V}_{BD}^{(B12)} \Big|_{J_{ij}^B \rightarrow J_{ij}^R, \alpha_{**}^{(B12)} \rightarrow \alpha_{**}^{(R12)}}, \quad (23)$$

where the parameters $\alpha_{**}^{(**)}$ are detailed in the Appendix. The loop functions J_{ij}^F , J_{ij}^T , J_{ij}^B , and J_{ij}^R are given in refs. [83–85]. Nevertheless, due to the varying masses of the internal pseudoscalar meson fields in the SU(3) framework, we have employed the formulas $\bar{\Delta} = m_1^2 + (m_2^2 - m_1^2)x + q^2 x(x-1) - i\epsilon$ and $A = m_1^2 - \omega^2 + (m_2^2 - m_1^2)x + q^2 x(x-1) - i\epsilon$ (where m_1 and m_2 denote the masses of the internal pseudoscalar meson fields), as substitutes for the equivalent expressions outlined in ref. [85]. In addition, we take the scale $\lambda = 4\pi f_\pi$ in the loop functions. The parameter d denotes the dimension introduced in the dimensional regularization. Note that, to generate the effective potential, one must subtract the two-particle reducible contributions from the box diagrams. A detailed deduction, based on the principal value integral method, is provided in Appendix B of ref. [85].

The two-pseudoscalar-meson-exchange diagrams for the BD^* system at order $\mathcal{O}(\epsilon^2)$ are depicted in Fig. 3. The effective potentials arising from these diagrams are expressed as follows:

$$\mathcal{V}_{BD^*}^{(F21)} = \alpha_{\pi\pi}^{(F21)} \frac{1}{f_\pi^4} J_{22}^F(m_\pi, m_\pi) + \alpha_{KK}^{(F21)} \frac{1}{f_K^4} J_{22}^F(m_K, m_K), \quad (24)$$

$$\mathcal{V}_{BD^*}^{(T21)} = \left\{ \frac{\alpha_{\pi\pi}^{(T21)}}{f_\pi^4}, \frac{\alpha_{KK}^{(T21)}}{f_K^4} \right\} g^2 \frac{(d-3)(d-2)}{d-1} \left[(d-1)J_{34}^T - (J_{24}^T + J_{33}^T) \mathbf{q}^2 \right] \{ (m_\pi, m_\pi), (m_K, m_K) \}, \quad (25)$$

$$\mathcal{V}_{BD^*}^{(T22)} = \left\{ \frac{\alpha_{\pi\pi}^{(T22)}}{f_\pi^4}, \frac{\alpha_{KK}^{(T22)}}{f_K^4} \right\} g^2 \left[J_{34}^T - \frac{1}{d-1} (J_{24}^T + J_{33}^T) \mathbf{q}^2 \right] \{ (m_\pi, m_\pi, \delta_D), (m_K, m_K, \delta_D) \}, \quad (26)$$

$$\mathcal{V}_{BD^*}^{(T23)} = \left\{ \frac{\alpha_{\pi\pi}^{(T23)}}{f_\pi^4}, \frac{\alpha_{KK}^{(T23)}}{f_K^4} \right\} \left[(d-1)J_{34}^T - (J_{24}^T + J_{33}^T) \mathbf{q}^2 \right] \{ (m_\pi, m_\pi), (m_K, m_K) \}, \quad (27)$$

$$\mathcal{V}_{BD^*}^{(T24)} = \left\{ \frac{\alpha_{\pi\pi}^{(T24)}}{f_\pi^4}, \frac{\alpha_{KK}^{(T24)}}{f_K^4} \right\} \left[(2-d)J_{34}^T - \frac{2-d}{d-1} (J_{24}^T + J_{33}^T) \mathbf{q}^2 \right] \{ (m_\pi, m_\pi, -\delta_B), (m_K, m_K, -\delta_B) \}, \quad (28)$$

$$\begin{aligned}
\mathcal{V}_{BD^*}^{(B21)} = & \left\{ \frac{\alpha_{\pi\pi}^{(B21)}}{f_\pi^4}, \frac{\alpha_{KK}^{(B21)}}{f_K^4}, \frac{\alpha_{\eta\eta}^{(B21)}}{f_\eta^4}, \frac{\alpha_{\pi\eta}^{(B21)}}{f_\pi^2 f_\eta^2}, \frac{\alpha_{\eta\pi}^{(B21)}}{f_\eta^2 f_\pi^2} \right\} g^2 \frac{(d-3)(d-2)}{d-1} \left\{ (d^2-1)J_{41}^B \right. \\
& - \left[\left(\frac{1}{d-2} \boldsymbol{\sigma} \cdot \mathbf{T} + 1 \right) J_{21}^B + 2(d+1)(J_{31}^B + J_{42}^B) \right] \mathbf{q}^2 + (J_{22}^B + 2J_{32}^B + J_{43}^B) \mathbf{q}^4 \left. \right\} \{ (m_\pi, m_\pi), \\
& (m_K, m_K), (m_\eta, m_\eta), (m_\pi, m_\eta), (m_\eta, m_\pi) \}, \tag{29}
\end{aligned}$$

$$\begin{aligned}
\mathcal{V}_{BD^*}^{(B22)} = & \left\{ \frac{\alpha_{\pi\pi}^{(B22)}}{f_\pi^4}, \frac{\alpha_{KK}^{(B22)}}{f_K^4}, \frac{\alpha_{\eta\eta}^{(B22)}}{f_\eta^4}, \frac{\alpha_{\pi\eta}^{(B22)}}{f_\pi^2 f_\eta^2}, \frac{\alpha_{\eta\pi}^{(B22)}}{f_\eta^2 f_\pi^2} \right\} \frac{g^2}{d-1} \left\{ (d^2-1)J_{41}^B + (J_{22}^B + 2J_{32}^B + J_{43}^B) \mathbf{q}^4 \right. \\
& - \left[(\boldsymbol{\sigma} \cdot \mathbf{T} + 1) J_{21}^B + 2(d+1)(J_{31}^B + J_{42}^B) \right] \mathbf{q}^2 \left. \right\} \{ (m_\pi, m_\pi, \delta_D), (m_K, m_K, \delta_D), \\
& (m_\eta, m_\eta, \delta_D), (m_\pi, m_\eta, \delta_D), (m_\eta, m_\pi, \delta_D) \}, \tag{30}
\end{aligned}$$

$$\begin{aligned}
\mathcal{V}_{BD^*}^{(B23)} = & \left\{ \frac{\alpha_{\pi\pi}^{(B23)}}{f_\pi^4}, \frac{\alpha_{KK}^{(B23)}}{f_K^4}, \frac{\alpha_{\eta\eta}^{(B23)}}{f_\eta^4}, \frac{\alpha_{\pi\eta}^{(B23)}}{f_\pi^2 f_\eta^2}, \frac{\alpha_{\eta\pi}^{(B23)}}{f_\eta^2 f_\pi^2} \right\} g^2 \mathcal{C}^2 \frac{(d-3)(d-2)^2}{(d-1)^2} \left\{ (d^2-1)J_{41}^B + (J_{22}^B + \right. \\
& 2J_{32}^B + J_{43}^B) \mathbf{q}^4 + \left[\frac{\boldsymbol{\sigma} \cdot \mathbf{T}}{(d-2)^2} J_{21}^B - J_{21}^B - 2(d+1)(J_{31}^B + J_{42}^B) \right] \mathbf{q}^2 \left. \right\} \{ (m_\pi, m_\pi, -\delta_B), \\
& (m_K, m_K, -\delta_B), (m_\eta, m_\eta, -\delta_B), (m_\pi, m_\eta, -\delta_B), (m_\eta, m_\pi, -\delta_B) \}, \tag{31}
\end{aligned}$$

$$\begin{aligned}
\mathcal{V}_{BD^*}^{(B24)} = & \left\{ \frac{\alpha_{\pi\pi}^{(B24)}}{f_\pi^4}, \frac{\alpha_{KK}^{(B24)}}{f_K^4}, \frac{\alpha_{\eta\eta}^{(B24)}}{f_\eta^4}, \frac{\alpha_{\pi\eta}^{(B24)}}{f_\pi^2 f_\eta^2}, \frac{\alpha_{\eta\pi}^{(B24)}}{f_\eta^2 f_\pi^2} \right\} g^2 \mathcal{C}^2 \frac{d-2}{(d-1)^2} \left\{ (J_{22}^B + 2J_{32}^B + J_{43}^B) \mathbf{q}^4 \right. \\
& + (d^2-1)J_{41}^B + \left[\left(\frac{\boldsymbol{\sigma} \cdot \mathbf{T}}{d-2} - 1 \right) J_{21}^B - 2(d+1)(J_{31}^B + J_{42}^B) \right] \mathbf{q}^2 \left. \right\} \{ (m_\pi, m_\pi, -\delta_B, \delta_D), \\
& (m_K, m_K, -\delta_B, \delta_D), (m_\eta, m_\eta, -\delta_B, \delta_D), (m_\pi, m_\eta, -\delta_B, \delta_D), (m_\eta, m_\pi, -\delta_B, \delta_D) \}, \tag{32}
\end{aligned}$$

$$\mathcal{V}_{BD^*}^{(R21)} = \mathcal{V}_{BD^*}^{(B21)} \Big|_{J_{ij}^B \rightarrow J_{ij}^R, \alpha_{**}^{(B21)} \rightarrow \alpha_{**}^{(R21)}, \boldsymbol{\sigma} \cdot \mathbf{T} \rightarrow -\boldsymbol{\sigma} \cdot \mathbf{T}}, \tag{33}$$

$$\mathcal{V}_{BD^*}^{(R22)} = \mathcal{V}_{BD^*}^{(B22)} \Big|_{J_{ij}^B \rightarrow J_{ij}^R, \alpha_{**}^{(B22)} \rightarrow \alpha_{**}^{(R22)}, \boldsymbol{\sigma} \cdot \mathbf{T} \rightarrow -\boldsymbol{\sigma} \cdot \mathbf{T}}, \tag{34}$$

$$\mathcal{V}_{BD^*}^{(R23)} = \mathcal{V}_{BD^*}^{(B23)} \Big|_{J_{ij}^B \rightarrow J_{ij}^R, \alpha_{**}^{(B23)} \rightarrow \alpha_{**}^{(R23)}, \boldsymbol{\sigma} \cdot \mathbf{T} \rightarrow -\boldsymbol{\sigma} \cdot \mathbf{T}}, \tag{35}$$

$$\mathcal{V}_{BD^*}^{(R24)} = \mathcal{V}_{BD^*}^{(B24)} \Big|_{J_{ij}^B \rightarrow J_{ij}^R, \alpha_{**}^{(B24)} \rightarrow \alpha_{**}^{(R24)}, \boldsymbol{\sigma} \cdot \mathbf{T} \rightarrow -\boldsymbol{\sigma} \cdot \mathbf{T}}, \tag{36}$$

where the parameters $\alpha_{**}^{(**)}$ are also detailed in the Appendix. In the above expressions, all physical quantities are defined in d dimensions, such as $\mathcal{S}^2 = (d-1)/4$ and $q_i q_j = 1/(d-1) \mathbf{q}^2 \delta_{ij}$ for the S wave.

At the next-to-leading order, in addition to the previously mentioned two-pseudoscalar-meson-exchange potentials, there exist one-loop corrections pertaining to the one-pseudoscalar-meson-exchange and contact terms. These one-loop corrections can be incorporated by substituting the physical values of relevant parameters such as the couplings, decay constant, and masses of light-mesons, baryons, and heavy-mesons. Furthermore, we also have the corrections from the subleading contact Lagrangians involving some unrenormalized $\mathcal{O}(\epsilon^2)$ LECs. In contrast to the nucleon-nucleon case, the current unavailability of baryon and heavy-meson scattering data impedes the fitting of these $\mathcal{O}(\epsilon^2)$ LECs. Consequently, we refrain from including their contributions and focus solely on the leading-order contact terms. Once the lattice QCD simulations provide access to the baryon and heavy meson scattering phase shifts, revisiting these systems while incorporating higher-order contributions would be an intriguing and worthwhile avenue for exploration.

Utilizing the momentum-space potentials $\mathcal{V}(\mathbf{q})$ derived above, we proceed with the subsequent Fourier transformation to acquire the effective potential $V(r)$ in coordinate space,

$$V(\mathbf{r}) = \int \frac{d^3 \mathbf{q}}{(2\pi)^3} e^{i\mathbf{q} \cdot \mathbf{r}} \mathcal{V}(\mathbf{q}) \mathcal{F}(\mathbf{q}). \tag{37}$$

In this context, the introduction of a regulator function $\mathcal{F}(\mathbf{q})$ becomes essential to suppress the high momentum contributions. For this purpose, we opt for the Gaussian form $\mathcal{F}(\mathbf{q}) = \exp(-\mathbf{q}^{2n}/\Lambda^{2n})$, previously utilized in studies related to the NN and $N\bar{N}$ systems [108–110]. The Taylor expansion of this regulator function can be expressed as $\mathcal{F}(\mathbf{q}) = 1 - \mathbf{q}^{2n}/\Lambda^{2n} + \dots$. The choice of the power n is crucial to ensure that the contributions from the cutoff-induced terms, $\mathcal{V}(\mathbf{q})\mathcal{O}(\mathbf{q}^{2n}/\Lambda^{2n})$, lie beyond the chiral order at which the analysis is conducted. Although our calculations primarily focus on the leading and subleading contributions, choosing $n = 1$ would suffice. However, for consistency with the estimation of the LECs in the $N\bar{N}$ system [110], where $n = 3$ was adopted, we also select $n = 3$. For the cutoff parameter Λ , we can make adjustments within the range of 400–600 MeV, guided by insights from alternative analyses [86, 87, 110–113].

Notably, due to $\delta_D > m_\pi$, certain diagrams in Fig. 3, specifically (T22) and (B22), would yield imaginary components, influencing the width of the associated bound state. If one were to solve the Lippmann-Schwinger equation, the presence of these imaginary parts would alter the pole position within the Riemann sheet. In this work, we opt for solving the Schrödinger equation, with a primary focus on the binding energies. Consequently, the imaginary components are disregarded in our calculations.

4 Results and discussion

To derive the numerical results, the LECs (D_a, D_b, E_a, E_b) need to be determined. Following the methodology proposed in ref. [86, 87, 91], we estimate the LECs through the development of a contact Lagrangian at the quark level. This involves the coupling constants c_s and c_t . The relationships ($D_a = 3c_s, D_b = -c_t, E_a = 3c_s, E_b = -5c_t$) were deduced by aligning the ND^* potentials from the hadron and quark levels in the SU(2) framework, as detailed in ref. [91]. Similarly, for the SU(3) framework, the relationships are established as ($D_a = 2c_s, D_b = 2c_t/3, E_a = 3c_s, E_b = -5c_t$). The values of c_s and c_t are derived from the $N\bar{N}$ interaction, as detailed in refs. [91, 110]. In this work, we adopt $c_s = -8.1 \text{ GeV}^{-2}$ and $c_t = 0.65 \text{ GeV}^{-2}$, as sourced from the Appendix of ref. [91].

Furthermore, we use the average values for the isospin multiplet masses of mesons and baryons from PDG [1]: $m_\pi = 137.27 \text{ MeV}$, $m_K = 495.64 \text{ MeV}$, $m_\eta = 547.86 \text{ MeV}$, $M_D = 1867.24 \text{ MeV}$, $M_{D_s} = 1968.34 \text{ MeV}$, $M_{D^*} = 2008.55 \text{ MeV}$, $M_{D_s^*} = 2112.20 \text{ MeV}$, $M_N = 938.92 \text{ MeV}$, $M_\Sigma = 1193.15 \text{ MeV}$, $M_\Xi = 1318.28 \text{ MeV}$, $M_\Lambda = 1115.68 \text{ MeV}$, $M_\Delta = 1232.00 \text{ MeV}$, $M_{\Sigma^*} = 1384.57 \text{ MeV}$, $M_{\Xi^*} = 1533.40 \text{ MeV}$, $M_\Omega = 1672.45 \text{ MeV}$. We also consider the average values for the mass differences: $\delta_B = 314.10 \text{ MeV}$ and $\delta_D = 142.59 \text{ MeV}$. The physical values of the pseudoscalar decay constants, as reported in PDG, are used: $f_\pi = 92.07 \text{ MeV}$, $f_K = 110.03 \text{ MeV}$, and $f_\eta = 1.2f_\pi$. The axial vector coupling constant g_A has been determined to be approximately 1.27, based on lattice quantum chromodynamics calculations [114] and measurements in the decay of free neutrons [115]. Accordingly, we adopt $D = 0.80$ and $F = 0.47$ as their physical values. These parameters are crucial for obtaining accurate numerical results in our theoretical framework.

In our analysis, we adopt $\mathcal{C} = 1.2$ based on the study of strong and electromagnetic decays of decuplet baryons, as detailed in ref. [116]. The coupling constant $g = -0.59$ is determined from the decay width of D^{*+} , as reported in refs. [117, 118]. The negative sign for g is derived using insights from the quark model. Regarding the cutoff parameter Λ , an extensive discussion is presented in ref. [91]. The findings from this reference suggest that a cutoff value of $\Lambda = 0.4 \text{ GeV}$ is suitable for accurately describing bound states. On the other hand, a higher cutoff value, such as $\Lambda = 0.6 \text{ GeV}$, is considered highly unnatural within the context of our calculation. Consequently, for the purpose of making predictions, we opt for $\Lambda = 0.4 \text{ GeV}$. This choice is informed by the need to ensure consistency and accuracy in our theoretical framework and the corresponding results.

4.1 $D_{(s)}^{(*)}N$ systems

We first analyze the D -meson and nucleon systems. The effective potentials of each possible IJ^P configuration are shown in Fig. 4. For the $[DN]_{J=1/2}^{I=0}$ system, the $\mathcal{O}(\epsilon^0)$ contact and $\mathcal{O}(\epsilon^2)$ two-meson-exchange potentials are both attractive. However, the attraction of the two-meson-exchange potentials is relatively weak. The dominant source of the attractive potential arises from the contact interaction. For the $[DN]_{J=1/2}^{I=1}$ and $[D_s N]_{J=1/2}^{I=1/2}$ systems, the $\mathcal{O}(\epsilon^0)$ contact interactions vanish in our calculation, and the total potentials stem from the two-meson-exchange

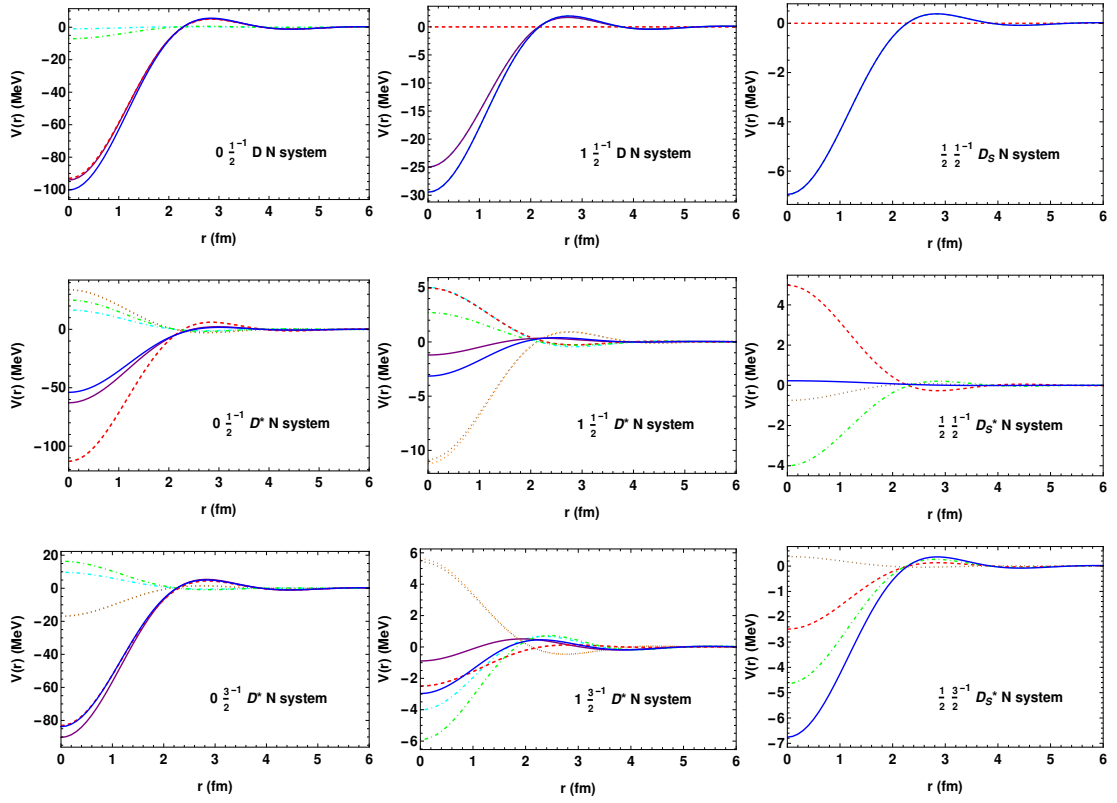


Figure 4: The effective potentials of the $D_{(s)}^{(*)}N$ systems. Their quantum numbers (IJ^P) are indicated in each subfigure. The red-dashed, brown-dotted, green-dotted-dashed, blue-solid lines denote the contact, one-meson-exchange, two-meson-exchange, and their total potentials in SU(3) framework, respectively. Meanwhile, the pink-dashed, orange-dotted, cyan-dotted-dashed, purple-solid lines present the contact, one-meson-exchange, two-meson-exchange, and their total potentials in SU(2) framework, respectively.

contributions. Notably, the potentials in the two channels exhibit considerably shallower depths when compared to the $[DN]_{J=1/2}^{I=0}$ channel, with a particular emphasis on the $[D_s N]_{J=1/2}^{I=1/2}$ channel.

In the $[D^*N]_{J=1/2}^{I=0}$ system, the contact interaction exhibits an attractive potential, while both the one-meson-exchange and two-meson-exchange potentials are repulsive. Despite this, the total potential of the system maintains approximately half the depth compared to that observed in the $[DN]_{J=1/2}^{I=0}$ channel. For the channel $[D^*N]_{J=3/2}^{I=0}$, the behavior of its potentials is intriguing. It is noteworthy that the contributions from one-meson-exchange and two-meson-exchange nearly offset each other. Consequently, the total potential is predominantly determined by the contact term, reaching a maximum depth of -80 MeV. In the $[D^*N]_{J=1/2}^{I=1}$, $[D^*N]_{J=3/2}^{I=1}$, $[D_s^*N]_{J=1/2}^{I=1/2}$, and $[D_s^*N]_{J=3/2}^{I=1/2}$ systems, the contact, one-meson-exchange, and two-meson-exchange potentials exhibit weakly attractive or weakly repulsive behavior. Consequently, their total potentials are also either weakly attractive or weakly repulsive.

In the $[DN]_{J=1/2}^{I=0,1}$ and $[D^*N]_{J=1/2,3/2}^{I=0,1}$ channels, we present the potentials arising from the SU(2) framework, where the η - and K -exchange contributions are excluded. In both the SU(2) and SU(3) frameworks, the contact and one-meson potentials exhibit nearly identical characteristics, while a small distinction emerges in the two-meson potentials. The total potentials from the SU(3) and SU(2) frameworks are not significantly different. Therefore, our calculation in SU(3) framework is reasonable.

We obtain the binding solutions in the $[DN]_{J=1/2}^{I=0}$, $[D^*N]_{J=1/2}^{I=0}$, and $[D^*N]_{J=3/2}^{I=0}$ systems, and the results are detailed in Table 1. Notably, the binding energy values for the SU(2) framework exhibit slight deviations from those reported in ref. [91]. This discrepancy primarily arises from our selection of different constants, particularly a smaller coupling constants for the $\Delta N\pi$ vertex. A key point of interest is the $[D^*N]_{J=3/2}^{I=0}$ channel. The mass of this bound state in the SU(3) framework closely aligns with the $\Lambda_c(2940)$ mass measurements.

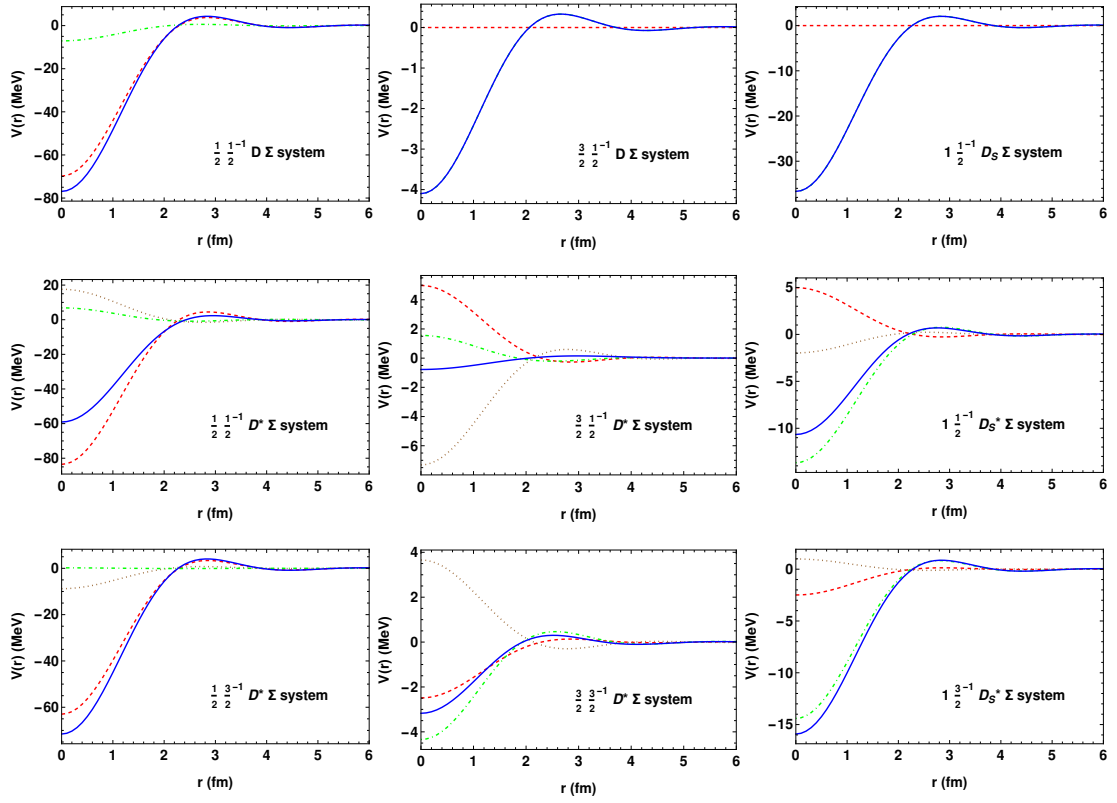


Figure 5: The effective potentials of the $D_{(s)}^{(*)}\Sigma$ systems. The notation is the same as in Fig. 4.

4.2 $D_{(s)}^{(*)}\Sigma$ systems

We then examine the D -meson and Σ -baryon systems. The effective potentials corresponding to each possible IJ^P configuration are depicted in Fig. 5. The features of $D\Sigma$ are very similar to those of DN , with the distinction that the effective potential of $[D_s\Sigma]_{J=1/2}^{I=1/2}$ is deeper than that of $[D\Sigma]_{J=1/2}^{I=3/2}$, while the effective potential of $[D_sN]_{J=1/2}^{I=1/2}$ is shallower than that of $[DN]_{J=1/2}^{I=1/2}$. This discrepancy is anticipated, given the presence of an attractive $s\bar{s}$ quark pair in $[D_s\Sigma]_{J=1/2}^{I=1/2}$. Despite the effective potential of $[D\Sigma]_{J=1/2}^{I=1/2}$ being slightly shallower than that of $[DN]_{J=1/2}^{I=0}$, it remains sufficiently deep to facilitate the formation of a bound state.

The characteristics of the $D^*\Sigma$ system show a striking similarity to those of the D^*N system. For the low-isospin channels, $[D^*\Sigma]_{J=1/2,3/2}^{I=1/2}$, we observe significantly deep attractive potentials. Conversely, the high-isospin channels, $[D^*\Sigma]_{J=1/2,3/2}^{I=3/2}$, as well as the strange channels $[D_s^*\Sigma]_{J=1/2,3/2}^{I=1/2}$, are characterized by shallower attractive potentials. In the case of the $[D^*\Sigma]_{J=1/2}^{I=1/2}$ system, there is an attractive contact interaction, although both one-meson-exchange and two-meson-exchange potentials are repulsive. This particular trait mirrors that of the $[D^*N]_{J=1/2}^{I=0}$

Table 1: The bound states for the $D_{(s)}^{(*)}N$ systems in SU(2) and SU(3) frameworks. The ΔE , M , and $\sqrt{\langle r^2 \rangle}$ denote the binding energy, the mass of the bound state, and the root mean square radius, respectively.

SU(3)/SU(2)	$[DN]_{J=1/2}^{I=0}$	$[D^*N]_{J=1/2}^{I=0}$	$[D^*N]_{J=3/2}^{I=0}$
ΔE (MeV)	-12.9/-10.5	-1.3/-2.9	-6.9/-9.3
M (MeV)	2793.2/2795.6	2946.2/2944.6	2940.5/2938.1
$\sqrt{\langle r^2 \rangle}$ (fm)	1.7/1.8	4.1/3.0	2.0/1.9

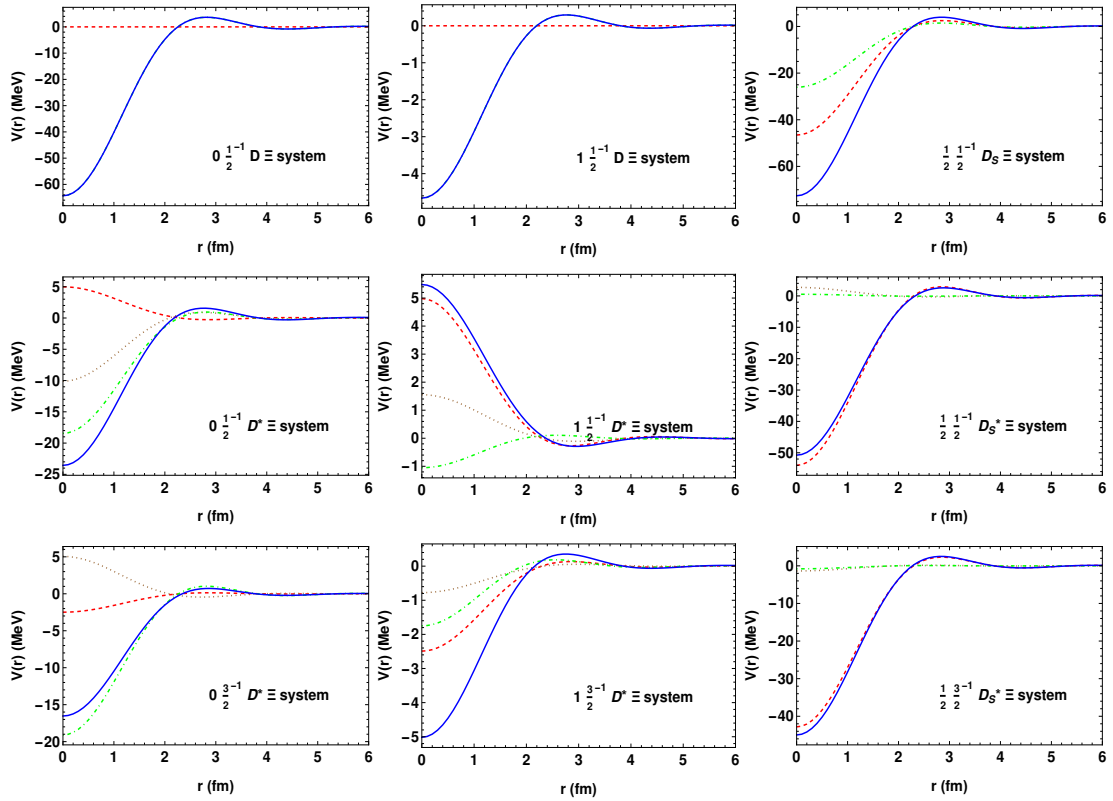


Figure 6: The effective potentials of the $D_{(s)}^{(*)}\Xi$ systems. The notation is the same as in Fig. 4.

system. In contrast, in the $[D^*\Sigma]_{J=3/2}^{I=1/2}$ system, the influence of the two-meson-exchange is negligible, diverging from the characteristics of the $[D^*N]_{J=3/2}^{I=0}$ system. Nevertheless, the attractive nature of the low-isospin channels is sufficient to facilitate the formation of bound states.

We also obtain binding solutions in the $[D\Sigma]_{J=1/2}^{I=1/2}$, $[D^*\Sigma]_{J=1/2}^{I=1/2}$, and $[D^*\Sigma]_{J=3/2}^{I=1/2}$ systems. The numerical results are presented in Table 2. It is evident that the bound states from $D^*\Sigma$ exhibit similarities to those from D^*N . The channel with low spin, $[D^*\Sigma]_{J=1/2}^{I=1/2}$, has a much shallower binding energy compared to the channel with high spin, $[D^*\Sigma]_{J=3/2}^{I=1/2}$. In analogy to interpreting $\Lambda_c(2940)$ as a molecular state of D^*N , we may propose to interpret the $\Xi_c(3196)$ as a bound state of $D^*\Sigma$ with $IJP = \frac{1}{2} \frac{3}{2}^-$ or $\frac{1}{2} \frac{1}{2}^-$. It is noteworthy that the molecular states also emerge in the $[D\Sigma]_{J=1/2}^{I=1/2}$ and $[D^*\Sigma]_{J=3/2}^{I=1/2}$ systems from the calculations in ref. [119]. Additionally, the $\Xi_c(3055)$ may be interpreted as the bound state of $[D\Sigma]_{J=1/2}^{I=1/2}$ system considering their nearly identical mass.

4.3 $D_{(s)}^{(*)}\Xi$ systems

We also investigate the systems composed of a D meson and a Ξ baryon. The effective potentials for each possible IJP configuration are illustrated in Fig. 6. A notable distinction emerges

Table 2: The bound states for the $D_{(s)}^{(*)}\Sigma$ systems in SU(3) framework. The notation is the same as in Table 1.

SU(3)	$[D\Sigma]_{J=1/2}^{I=1/2}$	$[D^*\Sigma]_{J=1/2}^{I=1/2}$	$[D^*\Sigma]_{J=3/2}^{I=1/2}$
ΔE (MeV)	-7.5	-3.6	-6.2
M (MeV)	3052.9	3198.1	3195.5
$\sqrt{\langle r^2 \rangle}$ (fm)	1.9	2.5	2.0

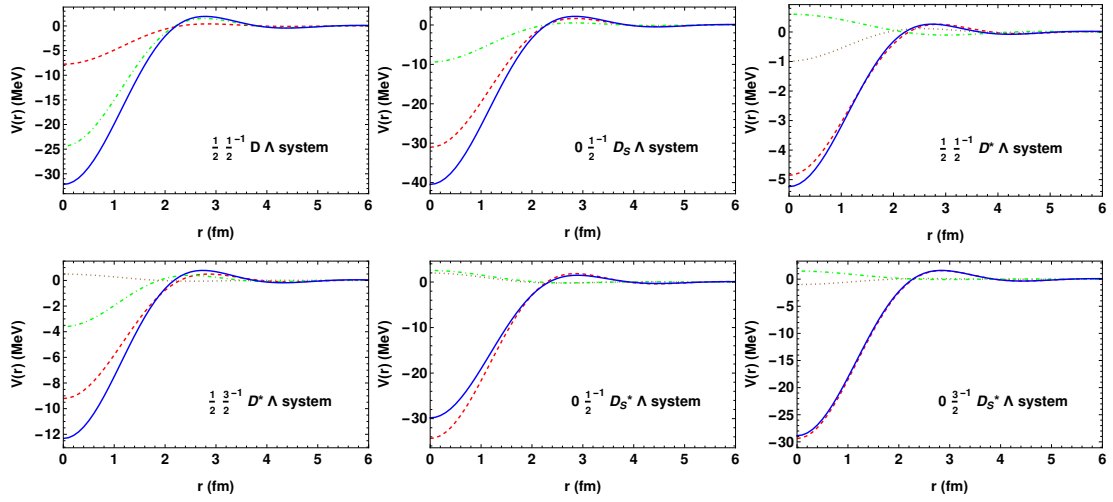


Figure 7: The effective potentials of the $D_{(s)}^{(*)}\Lambda$ systems. The notation is the same as in Fig. 4.

when comparing the characteristics of the $D\Xi$ systems to those of DN . Specifically, for the $[D\Xi]_{J=1/2}^{I=0}$ and $[D\Xi]_{J=1/2}^{I=1/2}$ systems, the $\mathcal{O}(\epsilon^0)$ contact interactions vanish in our calculation, since the total potentials are derived solely from the two-meson-exchange contributions. Conversely, in the $[D_s\Xi]_{J=1/2}^{I=1/2}$ system, the $\mathcal{O}(\epsilon^0)$ contact interaction is significant. This distinction leads to the emergence of sufficiently attractive potentials in the $[D\Xi]_{J=1/2}^{I=0}$ and $[D_s\Xi]_{J=1/2}^{I=1/2}$ systems, potentially indicating the formation of bound states. Meanwhile, a modestly attractive potential is observed in the $[D\Xi]_{J=1/2}^{I=1}$ system.

The $D^*\Xi$ system exhibits distinct characteristics compared to the D^*N system. In the low-isospin channels, specifically $[D^*\Xi]_{J=1/2,3/2}^{I=0}$, we detect attractive potentials. However, these potentials are not sufficiently deep to facilitate the formation of bound states. Conversely, in the high-isospin channels, $[D^*\Xi]_{J=1/2,3/2}^{I=1}$, we observe a mixture of shallower repulsive and attractive potentials. With regard to the $[D_s^*\Xi]_{J=1/2,3/2}^{I=1/2}$ systems, both the one-meson-exchange and two-meson-exchange potentials appear relatively weak. Notably, the primary source of the attractive potential in these cases stem from the contact interactions. Despite the total potentials are not profoundly deep, they are sufficiently strong to potentially lead to the formation of bound states.

We obtain binding solutions in the $[D\Xi]_{J=1/2}^{I=0}$, $[D_s\Xi]_{J=1/2}^{I=1/2}$, $[D_s^*\Xi]_{J=1/2}^{I=1/2}$, and $[D_s^*\Xi]_{J=3/2}^{I=1/2}$ systems, with comprehensive results detailed in Table 3. Notably, the bound state associated with the $[D_s^*\Xi]_{J=1/2,3/2}^{I=1/2}$ system may correspond to the $\Xi_c(3429)$. Furthermore, the $\Xi_c(3279)$ may be interpreted as the bound state of the $[D_s\Xi]_{J=1/2}^{I=1/2}$. Intriguingly, its mass closely aligns with that of the bound state in the $[D^*\Sigma]_{J=1/2}^{I=1/2}$ system, and they share identical quantum numbers. These two channels may be considered as the coupled-channels. Additionally, the bound state in the $[D\Xi]_{J=1/2}^{I=0}$ system may correspond to the $\Omega_c(3188)$ observed by LHCb [120]. Our result for this channel is in agreement with ref. [121], where a bound state was identified. However, it contrasts with the findings in refs. [119, 122], in which a $2S$ Ω_c -baryon and a virtual state were reported, respectively.

Table 3: The bound states for the $D_{(s)}^{(*)}\Xi$ systems in SU(3) framework. The notation is the same as in Table 1.

SU(3)	$[D\Xi]_{J=1/2}^{I=0}$	$[D_s\Xi]_{J=1/2}^{I=1/2}$	$[D_s^*\Xi]_{J=1/2}^{I=1/2}$	$[D_s^*\Xi]_{J=3/2}^{I=1/2}$
ΔE (MeV)	-4.1	-7.7	-1.7	-0.4
M (MeV)	3181.4	3279.0	3428.8	3430.1
$\sqrt{\langle r^2 \rangle}$ (fm)	2.3	1.9	3.2	5.7

4.4 $D_{(s)}^{(*)}\Lambda$ systems

Finally, we explore the D -meson and Λ -baryon systems. For each possible IJ^P configuration within these systems, we illustrate the effective potentials in Fig. 7. Compared with the previously discussed systems, it is noteworthy that all the $\mathcal{O}(\epsilon^0)$ contact interactions are nonvanishing here. However, these interactions are not sufficiently attractive to form bound states, even when taking into account both the one-meson-exchange and two-meson-exchange contributions. Particularly in the $[D_s\Lambda]_{J=1/2}^{I=0}$ system, we observe a significantly attractive contact potential coupled with an attractive two-meson-exchange potential, results in the most significant potential observed within the $D_{(s)}^{(*)}\Lambda$ systems. It is crucial to emphasize that no binding solution exists in these systems.

5 Summary

In this work, we have comprehensively calculated the effective potentials of the octet baryon and D -meson systems up to the next-to-leading order using the chiral effective field theory. Our approach encompasses the long-range one-pseudoscalar-meson-exchange potential, the mid-range two-pseudoscalar-meson-exchange potential, and the short-range contact interactions. Additionally, we have incorporated the decuplet baryons as the intermediate states within the loop diagrams. The involved low energy constants are judiciously estimated based on the $N\bar{N}$ interaction with help of the quark model.

In our investigation of the $D_{(s)}^{(*)}N$ systems, we have almost obtained attractive potentials in all channels, with the exception of the $[D_s^*N]_{J=1/2}^{I=1/2}$ channel. Significantly, bound states emerge only in the $[DN]_{J=1/2}^{I=0}$, $[D^*N]_{J=1/2}^{I=0}$, and $[D^*N]_{J=3/2}^{I=0}$ systems, owing to the sufficient depth of their attractive potentials. Notably, the mass of the bound state in the $[D^*N]_{J=3/2}^{I=0}$ system exhibits a remarkable correspondence with the mass of the $\Lambda_c(2940)$.

In our examination of the $D_{(s)}^{(*)}\Sigma$ systems, we observe that their characteristics closely mirror those of the $D_{(s)}^{(*)}N$ systems. We have obtained attractive potentials in all channels. Specifically, bound states appear in the $[D\Sigma]_{J=1/2}^{I=1/2}$, $[D^*\Sigma]_{J=1/2}^{I=1/2}$, and $[D^*\Sigma]_{J=3/2}^{I=1/2}$ systems. The bound state in the $[D\Sigma]_{J=1/2}^{I=1/2}$ system notably aligns in mass with $\Xi_c(3055)$, suggesting its interpretation as a molecular state. The bound state corresponding to $D^*\Sigma$ leads to the molecular explanation of the $\Xi_c(3196)$. These two cases parallel the interpretation of $\Lambda_c(2940)$ as a molecular state of D^*N .

In our analysis of the $D_{(s)}^{(*)}\Xi$ systems, we observe distinct characteristics compared to the $D_{(s)}^{(*)}N$ systems. While a repulsive potential is identified in the $[D^*\Xi]_{J=1/2}^{I=1/2}$ channel, attractive potentials are present in the other channels. Significantly deep potentials, capable of generating bound states, are found in the $[D\Xi]_{J=1/2}^{I=0}$, $[D_s\Xi]_{J=1/2}^{I=1/2}$, $[D_s^*\Xi]_{J=1/2}^{I=1/2}$, $[D_s^*\Xi]_{J=3/2}^{I=1/2}$ systems. The bound state in the $[D\Xi]_{J=1/2}^{I=0}$ system may correspond to the $\Omega_c(3188)$. Moreover, the $\Xi_c(3279)$ and $\Xi_c(3429)$ may be interpreted as the molecular states of $[D_s\Xi]_{J=1/2}^{I=1/2}$ and $[D_s^*\Xi]_{J=1/2,3/2}^{I=1/2}$, respectively.

In our study of the $D_{(s)}^{(*)}\Lambda$ systems, attractive potentials are identified in all channels. Nevertheless, these attractive potentials are not sufficiently deep to facilitate the formation of bound states in any of these systems.

To summarize, our investigations provide new insights into the $\Lambda_c(2940)$, $\Xi_c(3055)$, and $\Omega_c(3188)$ states from the hadronic molecular perspective. We have also identified specific molecular states, designated as Ξ_c , within the mass range of 3100 – 3500 MeV. The further experimental measurements of their masses, widths, spin-parity quantum numbers and decay patterns will help to discriminate the conventional baryon and hadronic molecule explanations for these near-threshold states. We look forward with great anticipation to future experimental validation of the possible existence of the singly heavy molecular baryon states. Such findings would significantly enhance our comprehension of the molecular state dynamics in heavy quark systems.

Acknowledgments

This work is supported by the National Natural Science Foundation of China under Grants No. 11975033, No. 12070131001, No. 12147127, No. 12105072, and No. 12305090. B. Wang was also supported by the Youth Funds of Hebei Province (No. A2021201027) and the Start-up Funds for Young Talents of Hebei University (No. 521100221021). We thank Zi-Yang Lin (Peking University), Lu Meng (Ruhr-Universität Bochum) for very helpful discussions.

A Parameters for the potentials

This appendix details the parameters for the potentials, as shown in Tables [A.1](#) to [A.2](#) below.

Table A.1: Parameters for the potentials of the BD or BD^* systems.

Systems	$ND^{(*)}(I=1)$	$ND^{(*)}(I=0)$	$ND_S^{(*)}(I=\frac{1}{2})$	$\Sigma D^{(*)}(I=\frac{3}{2})$	$\Sigma D^{(*)}(I=\frac{1}{2})$	$\Sigma D_S^{(*)}(I=1)$	$\Xi D^{(*)}(I=1)$	$\Xi D^{(*)}(I=0)$	$\Xi D_S^{(*)}(I=\frac{1}{2})$	$\Lambda D^{(*)}(I=\frac{1}{2})$	$\Lambda D_S^{(*)}(I=0)$
$\alpha^{(X11)}/\alpha^{(X21)}$	$-\frac{2}{3}$	$\frac{10}{3}$	$-\frac{2}{3}$	$-\frac{2}{3}$	$\frac{7}{3}$	$-\frac{2}{3}$	$-\frac{2}{3}$	$-\frac{2}{3}$	$\frac{4}{3}$	$-\frac{1}{3}$	$\frac{2}{3}$
$\alpha_\pi^{(H21)}$	$\frac{D+F}{4}$	$-\frac{3}{4}(D+F)$	0	$\frac{F}{2}$	$-F$	0	$\frac{F-D}{4}$	$\frac{3(D-F)}{4}$	0	0	0
$\alpha_\eta^{(H21)}$	$\frac{1}{12}(D-3F)$	$\frac{1}{12}(D-3F)$	$\frac{1}{6}(3F-D)$	$-\frac{D}{6}$	$-\frac{D}{6}$	$\frac{D}{3}$	$\frac{1}{12}(D+3F)$	$\frac{1}{12}(D+3F)$	$\frac{1}{6}(-D-3F)$	$\frac{D}{6}$	$-\frac{D}{3}$
$\alpha_{\pi\pi}^{(F11)}/\alpha_{\pi\pi}^{(F21)}$	$\frac{1}{4}$	$-\frac{3}{4}$	0	$\frac{1}{2}$	-1	0	$\frac{1}{4}$	$-\frac{3}{4}$	0	0	0
$\alpha_{KK}^{(F11)}/\alpha_{KK}^{(F21)}$	$-\frac{3}{16}$	$-\frac{9}{16}$	$\frac{11}{16}$	$\frac{3}{16}$	$-\frac{3}{8}$	$\frac{1}{16}$	$\frac{3}{8}$	0	$-\frac{5}{8}$	0	0
$\alpha_{\pi\pi}^{(T11)}$	$\frac{1}{4}$	$-\frac{3}{4}$	0	$\frac{1}{2}$	-1	0	$\frac{1}{4}$	$-\frac{3}{4}$	0	0	0
$\alpha_{KK}^{(T11)}$	$-\frac{1}{4}$	$-\frac{3}{4}$	$\frac{3}{4}$	$\frac{1}{4}$	$-\frac{1}{2}$	0	$\frac{1}{2}$	0	$-\frac{3}{4}$	0	0
$\alpha_{\pi\pi}^{(T12)}/\alpha_{\pi\pi}^{(T24)}$	$\frac{1}{6}$	$-\frac{1}{2}$	0	$-\frac{1}{24}$	$\frac{1}{12}$	0	$-\frac{1}{12}$	$\frac{1}{4}$	0	0	0
$\alpha_{KK}^{(T12)}/\alpha_{KK}^{(T24)}$	$\frac{1}{12}$	0	$-\frac{1}{8}$	$-\frac{1}{12}$	$-\frac{5}{24}$	$\frac{1}{4}$	$-\frac{1}{24}$	$\frac{3}{8}$	$-\frac{1}{8}$	$\frac{1}{8}$	$-\frac{1}{4}$
$\alpha_{\pi\pi}^{(T13)}/\alpha_{\pi\pi}^{(T23)}$	$\frac{1}{4}(D+F)^2$	$-\frac{3}{4}(D+F)^2$	0	$\frac{1}{6}(D^2+3F^2)$	$-\frac{D^2}{3}-F^2$	0	$\frac{1}{4}(D-F)^2$	$-\frac{3}{4}(D-F)^2$	0	0	0
$\alpha_{KK}^{(T13)}/\alpha_{KK}^{(T23)}$	$-\frac{1}{4}(D-F)^2$	$-\frac{1}{12}(D+3F)^2$	$\frac{1}{12}(5D^2-6DF+9F^2)$	$\frac{1}{4}(D-F)^2$	$\frac{1}{2}(-D^2-DF-F^2)$	DF	$\frac{1}{6}(D^2+3F^2)$	$\frac{1}{3}D(D+3F)$	$\frac{1}{12}(-5D^2-6DF-9F^2)$	$\frac{DF}{2}$	$-DF$
$\alpha_{\pi\pi}^{(B11)}$	$\frac{1}{16}(D+F)^2$	$\frac{9}{16}(D+F)^2$	0	$\frac{F^2}{4}$	$\frac{D^2}{4}+F^2$	0	$\frac{1}{16}(D-F)^2$	$\frac{9}{16}(D-F)^2$	0	$\frac{D^2}{4}$	0
$\alpha_{KK}^{(B11)}$	$\frac{1}{4}(D-F)^2$	$\frac{1}{12}(D+3F)^2$	0	0	$\frac{3}{8}(D+F)^2$	$\frac{1}{4}(D-F)^2$	0	0	$\frac{1}{12}(5D^2+6DF+9F^2)$	$\frac{1}{24}(D-3F)^2$	$\frac{1}{12}(D+3F)^2$
$\alpha_{\eta\eta}^{(B11)}$	$\frac{1}{144}(D-3F)^2$	$\frac{1}{144}(D-3F)^2$	$\frac{1}{36}(D-3F)^2$	$\frac{D^2}{36}$	$\frac{D^2}{36}$	$\frac{D^2}{9}$	$\frac{1}{144}(D+3F)^2$	$\frac{1}{144}(D+3F)^2$	$\frac{1}{36}(D+3F)^2$	$\frac{D^2}{36}$	$\frac{D^2}{9}$
$\alpha_{\pi\eta}^{(B11)}/\alpha_{\eta\pi}^{(B11)}$	$\frac{1}{48}(D-3F)(D+F)$	$-\frac{1}{16}(D-3F)(D+F)$	0	$-\frac{DF}{12}$	$\frac{DF}{6}$	0	$-\frac{1}{48}(D-F)(D+3F)$	$\frac{1}{16}(D-F)(D+3F)$	0	0	0
$\alpha_{\pi\pi}^{(B12)}$	$\frac{1}{3}$	0	0	$\frac{1}{48}$	$\frac{1}{12}$	0	$\frac{1}{48}$	$\frac{3}{16}$	0	$\frac{3}{16}$	0
$\alpha_{KK}^{(B12)}$	$\frac{1}{12}$	0	0	0	$\frac{1}{8}$	$\frac{1}{3}$	0	$\frac{1}{2}$	$\frac{1}{8}$	$\frac{1}{8}$	0
$\alpha_{\eta\eta}^{(B12)}$	0	0	0	$\frac{1}{48}$	$\frac{1}{48}$	$\frac{1}{12}$	$\frac{1}{48}$	$\frac{1}{48}$	$\frac{1}{12}$	0	0
$\alpha_{\pi\eta}^{(B12)}/\alpha_{\eta\pi}^{(B12)}$	0	0	0	$-\frac{1}{48}$	$\frac{1}{24}$	0	$-\frac{1}{48}$	$\frac{1}{16}$	0	0	0
$\alpha_{\pi\pi}^{(R11)}$	$\frac{5}{16}(D+F)^2$	$-\frac{3}{16}(D+F)^2$	0	$\frac{D^2}{6}+\frac{3F^2}{4}$	$-\frac{D^2}{12}$	0	$\frac{5}{16}(D-F)^2$	$-\frac{3}{16}(D-F)^2$	0	$\frac{D^2}{4}$	0
$\alpha_{KK}^{(R11)}$	0	0	$\frac{1}{12}(5D^2-6DF+9F^2)$	$\frac{1}{4}(D-F)^2$	$-\frac{1}{8}(D-F)^2$	$\frac{1}{4}(D+F)^2$	$\frac{1}{6}(D^2+3F^2)$	$\frac{1}{3}D(D+3F)$	0	$\frac{1}{24}(D+3F)^2$	$\frac{1}{12}(D-3F)^2$
$\alpha_{\eta\eta}^{(R11)}$	$\frac{1}{144}(D-3F)^2$	$\frac{1}{144}(D-3F)^2$	$\frac{1}{36}(D-3F)^2$	$\frac{D^2}{36}$	$\frac{D^2}{36}$	$\frac{D^2}{9}$	$\frac{1}{144}(D+3F)^2$	$\frac{1}{144}(D+3F)^2$	$\frac{1}{36}(D+3F)^2$	$\frac{D^2}{36}$	$\frac{D^2}{9}$
$\alpha_{\pi\eta}^{(R11)}/\alpha_{\eta\pi}^{(R11)}$	$\frac{1}{48}(D-3F)(D+F)$	$-\frac{1}{16}(D-3F)(D+F)$	0	$-\frac{DF}{12}$	$\frac{DF}{6}$	0	$-\frac{1}{48}(D-F)(D+3F)$	$\frac{1}{16}(D-F)(D+3F)$	0	0	0
$\alpha_{\pi\pi}^{(R12)}$	$\frac{1}{6}$	$\frac{1}{2}$	0	$\frac{1}{16}$	0	0	$\frac{5}{48}$	$-\frac{1}{16}$	0	$\frac{3}{16}$	0
$\alpha_{KK}^{(R12)}$	0	0	$\frac{1}{8}$	$\frac{1}{12}$	$\frac{1}{3}$	$\frac{1}{12}$	$\frac{1}{24}$	$\frac{1}{8}$	$\frac{1}{4}$	0	$\frac{1}{4}$
$\alpha_{\eta\eta}^{(R12)}$	0	0	0	$\frac{1}{48}$	$\frac{1}{48}$	$\frac{1}{12}$	$\frac{1}{48}$	$\frac{1}{48}$	$\frac{1}{12}$	0	0
$\alpha_{\pi\eta}^{(R12)}/\alpha_{\eta\pi}^{(R12)}$	0	0	0	$-\frac{1}{48}$	$\frac{1}{24}$	0	$-\frac{1}{48}$	$\frac{1}{16}$	0	0	0
$\alpha_{\pi\pi}^{(T21)}$	$\frac{1}{4}$	$-\frac{3}{4}$	0	$\frac{1}{2}$	-1	0	$\frac{1}{4}$	$-\frac{3}{4}$	0	0	0
$\alpha_{KK}^{(T21)}$	$-\frac{1}{4}$	$-\frac{3}{4}$	$\frac{3}{4}$	$\frac{1}{4}$	$-\frac{1}{2}$	0	$\frac{1}{2}$	0	$-\frac{3}{4}$	0	0
$\alpha_{\pi\pi}^{(T22)}$	$\frac{1}{4}$	$-\frac{3}{4}$	0	$\frac{1}{2}$	-1	0	$\frac{1}{4}$	$-\frac{3}{4}$	0	0	0
$\alpha_{KK}^{(T22)}$	$-\frac{1}{4}$	$-\frac{3}{4}$	$\frac{3}{4}$	$\frac{1}{4}$	$-\frac{1}{2}$	0	$\frac{1}{2}$	0	$-\frac{3}{4}$	0	0
$\alpha_{\pi\pi}^{(B21)}$	$\frac{1}{16}(D+F)^2$	$\frac{9}{16}(D+F)^2$	0	$\frac{F^2}{4}$	$\frac{D^2}{4}+F^2$	0	$\frac{1}{16}(D-F)^2$	$\frac{9}{16}(D-F)^2$	0	$\frac{D^2}{4}$	0

Table A.2: Continue.

Systems	$ND^{(*)}(I=1)$	$ND^{(*)}(I=0)$	$ND_S^{(*)}(I=\frac{1}{2})$	$\Sigma D^{(*)}(I=\frac{3}{2})$	$\Sigma D^{(*)}(I=\frac{1}{2})$	$\Sigma D_S^{(*)}(I=1)$	$\Xi D^{(*)}(I=1)$	$\Xi D^{(*)}(I=0)$	$\Xi D_S^{(*)}(I=\frac{1}{2})$	$\Lambda D^{(*)}(I=\frac{1}{2})$	$\Lambda D_S^{(*)}(I=0)$
$\alpha_{KK}^{(B21)}$	$\frac{1}{4}(D-F)^2$	$\frac{1}{12}(D+3F)^2$	0	0	$\frac{3}{8}(D+F)^2$	$\frac{1}{4}(D-F)^2$	0	0	$\frac{1}{12}(5D^2+6DF+9F^2)$	$\frac{1}{24}(D-3F)^2$	$\frac{1}{12}(D+3F)^2$
$\alpha_{\eta\eta}^{(B21)}$	$\frac{1}{144}(D-3F)^2$	$\frac{1}{144}(D-3F)^2$	$\frac{1}{36}(D-3F)^2$	$\frac{D^2}{36}$	$\frac{D^2}{36}$	$\frac{D^2}{9}$	$\frac{1}{144}(D+3F)^2$	$\frac{1}{144}(D+3F)^2$	$\frac{1}{36}(D+3F)^2$	$\frac{D^2}{36}$	$\frac{D^2}{9}$
$\alpha_{\pi\eta}^{(B21)}/\alpha_{\eta\pi}^{(B21)}$	$\frac{1}{48}(D-3F)(D+F)$	$-\frac{1}{16}(D-3F)(D+F)$	0	$-\frac{DF}{12}$	$\frac{DF}{6}$	0	$-\frac{1}{48}(D-F)(D+3F)$	$\frac{1}{16}(D-F)(D+3F)$	0	0	0
$\alpha_{\pi\pi}^{(B22)}$	$\frac{1}{16}(D+F)^2$	$\frac{9}{16}(D+F)^2$	0	$\frac{F^2}{4}$	$\frac{D^2}{4}+F^2$	0	$\frac{1}{16}(D-F)^2$	$\frac{9}{16}(D-F)^2$	0	$\frac{D^2}{4}$	0
$\alpha_{KK}^{(B22)}$	$\frac{1}{4}(D-F)^2$	$\frac{1}{12}(D+3F)^2$	0	0	$\frac{3}{8}(D+F)^2$	$\frac{1}{4}(D-F)^2$	0	0	$\frac{1}{12}(5D^2+6DF+9F^2)$	$\frac{1}{24}(D-3F)^2$	$\frac{1}{12}(D+3F)^2$
$\alpha_{\eta\eta}^{(B22)}$	$\frac{1}{144}(D-3F)^2$	$\frac{1}{144}(D-3F)^2$	$\frac{1}{36}(D-3F)^2$	$\frac{D^2}{36}$	$\frac{D^2}{36}$	$\frac{D^2}{9}$	$\frac{1}{144}(D+3F)^2$	$\frac{1}{144}(D+3F)^2$	$\frac{1}{36}(D+3F)^2$	$\frac{D^2}{36}$	$\frac{D^2}{9}$
$\alpha_{\pi\eta}^{(B22)}/\alpha_{\eta\pi}^{(B22)}$	$\frac{1}{48}(D-3F)(D+F)$	$-\frac{1}{16}(D-3F)(D+F)$	0	$-\frac{DF}{12}$	$\frac{DF}{6}$	0	$-\frac{1}{48}(D-F)(D+3F)$	$\frac{1}{16}(D-F)(D+3F)$	0	0	0
$\alpha_{\pi\pi}^{(B23)}$	$\frac{1}{3}$	0	0	$\frac{1}{48}$	$\frac{1}{12}$	0	$\frac{1}{48}$	$\frac{3}{16}$	0	$\frac{3}{16}$	0
$\alpha_{KK}^{(B23)}$	$\frac{1}{12}$	0	0	0	$\frac{1}{8}$	$\frac{1}{3}$	0	$\frac{1}{2}$	$\frac{1}{8}$	$\frac{1}{8}$	0
$\alpha_{\eta\eta}^{(B23)}$	0	0	0	$\frac{1}{48}$	$\frac{1}{48}$	$\frac{1}{12}$	$\frac{1}{48}$	$\frac{1}{48}$	$\frac{1}{12}$	0	0
$\alpha_{\pi\eta}^{(B23)}/\alpha_{\eta\pi}^{(B23)}$	0	0	0	$\frac{1}{48}$	$-\frac{1}{24}$	0	$\frac{1}{48}$	$-\frac{1}{16}$	0	0	0
$\alpha_{\pi\pi}^{(B24)}$	$\frac{1}{3}$	0	0	$\frac{1}{48}$	$\frac{1}{12}$	0	$\frac{1}{48}$	$\frac{3}{16}$	0	$\frac{3}{16}$	0
$\alpha_{KK}^{(B24)}$	$\frac{1}{12}$	0	0	0	$\frac{1}{8}$	$\frac{1}{3}$	0	$\frac{1}{2}$	$\frac{1}{8}$	$\frac{1}{8}$	0
$\alpha_{\eta\eta}^{(B24)}$	0	0	0	$\frac{1}{48}$	$\frac{1}{48}$	$\frac{1}{12}$	$\frac{1}{48}$	$\frac{1}{48}$	$\frac{1}{12}$	0	0
$\alpha_{\pi\eta}^{(B24)}/\alpha_{\eta\pi}^{(B24)}$	0	0	0	$-\frac{1}{48}$	$\frac{1}{24}$	0	$-\frac{1}{48}$	$\frac{1}{16}$	0	0	0
$\alpha_{\pi\pi}^{(R21)}$	$\frac{5}{16}(D+F)^2$	$-\frac{3}{16}(D+F)^2$	0	$\frac{D^2}{6}+\frac{3F^2}{4}$	$-\frac{D^2}{12}$	0	$\frac{5}{16}(D-F)^2$	$-\frac{3}{16}(D-F)^2$	0	$\frac{D^2}{4}$	0
$\alpha_{KK}^{(R21)}$	0	0	$\frac{1}{12}(5D^2-6DF+9F^2)$	$\frac{1}{4}(D-F)^2$	$-\frac{1}{8}(D-F)^2$	$\frac{1}{4}(D+F)^2$	$\frac{1}{6}(D^2+3F^2)$	$\frac{1}{3}D(D+3F)$	0	$\frac{1}{24}(D+3F)^2$	$\frac{1}{12}(D-3F)^2$
$\alpha_{\eta\eta}^{(R21)}$	$\frac{1}{144}(D-3F)^2$	$\frac{1}{144}(D-3F)^2$	$\frac{1}{36}(D-3F)^2$	$\frac{D^2}{36}$	$\frac{D^2}{36}$	$\frac{D^2}{9}$	$\frac{1}{144}(D+3F)^2$	$\frac{1}{144}(D+3F)^2$	$\frac{1}{36}(D+3F)^2$	$\frac{D^2}{36}$	$\frac{D^2}{9}$
$\alpha_{\pi\eta}^{(R21)}/\alpha_{\eta\pi}^{(R21)}$	$\frac{1}{48}(D-3F)(D+F)$	$-\frac{1}{16}(D-3F)(D+F)$	0	$-\frac{DF}{12}$	$\frac{DF}{6}$	0	$-\frac{1}{48}(D-F)(D+3F)$	$\frac{1}{16}(D-F)(D+3F)$	0	0	0
$\alpha_{\pi\pi}^{(R22)}$	$\frac{5}{16}(D+F)^2$	$-\frac{3}{16}(D+F)^2$	0	$\frac{D^2}{6}+\frac{3F^2}{4}$	$-\frac{D^2}{12}$	0	$\frac{5}{16}(D-F)^2$	$-\frac{3}{16}(D-F)^2$	0	$\frac{D^2}{4}$	0
$\alpha_{KK}^{(R22)}$	0	0	$\frac{1}{12}(5D^2-6DF+9F^2)$	$\frac{1}{4}(D-F)^2$	$-\frac{1}{8}(D-F)^2$	$\frac{1}{4}(D+F)^2$	$\frac{1}{6}(D^2+3F^2)$	$\frac{1}{3}D(D+3F)$	0	$\frac{1}{24}(D+3F)^2$	$\frac{1}{12}(D-3F)^2$
$\alpha_{\eta\eta}^{(R22)}$	$\frac{1}{144}(D-3F)^2$	$\frac{1}{144}(D-3F)^2$	$\frac{1}{36}(D-3F)^2$	$\frac{D^2}{36}$	$\frac{D^2}{36}$	$\frac{D^2}{9}$	$\frac{1}{144}(D+3F)^2$	$\frac{1}{144}(D+3F)^2$	$\frac{1}{36}(D+3F)^2$	$\frac{D^2}{36}$	$\frac{D^2}{9}$
$\alpha_{\pi\eta}^{(R22)}/\alpha_{\eta\pi}^{(R22)}$	$\frac{1}{48}(D-3F)(D+F)$	$-\frac{1}{16}(D-3F)(D+F)$	0	$-\frac{DF}{12}$	$\frac{DF}{6}$	0	$-\frac{1}{48}(D-F)(D+3F)$	$\frac{1}{16}(D-F)(D+3F)$	0	0	0
$\alpha_{\pi\pi}^{(R23)}$	$\frac{1}{6}$	$\frac{1}{2}$	0	$\frac{1}{16}$	0	0	$\frac{5}{48}$	$-\frac{1}{16}$	0	$\frac{3}{16}$	0
$\alpha_{KK}^{(R23)}$	0	0	$\frac{1}{8}$	$\frac{1}{12}$	$\frac{1}{3}$	$\frac{1}{12}$	$\frac{1}{24}$	$\frac{1}{8}$	$\frac{1}{4}$	0	$\frac{1}{4}$
$\alpha_{\eta\eta}^{(R23)}$	0	0	0	$\frac{1}{48}$	$\frac{1}{48}$	$\frac{1}{12}$	$\frac{1}{48}$	$\frac{1}{48}$	$\frac{1}{12}$	0	0
$\alpha_{\pi\eta}^{(R23)}/\alpha_{\eta\pi}^{(R23)}$	0	0	0	$\frac{1}{48}$	$-\frac{1}{24}$	0	$\frac{1}{48}$	$-\frac{1}{16}$	0	0	0
$\alpha_{\pi\pi}^{(R24)}$	$\frac{1}{6}$	$\frac{1}{2}$	0	$\frac{1}{16}$	0	0	$\frac{5}{48}$	$-\frac{1}{16}$	0	$\frac{3}{16}$	0
$\alpha_{KK}^{(R24)}$	0	0	$\frac{1}{8}$	$\frac{1}{12}$	$\frac{1}{3}$	$\frac{1}{12}$	$\frac{1}{24}$	$\frac{1}{8}$	$\frac{1}{4}$	0	$\frac{1}{4}$
$\alpha_{\eta\eta}^{(R24)}$	0	0	0	$\frac{1}{48}$	$\frac{1}{48}$	$\frac{1}{12}$	$\frac{1}{48}$	$\frac{1}{48}$	$\frac{1}{12}$	0	0
$\alpha_{\pi\eta}^{(R24)}/\alpha_{\eta\pi}^{(R24)}$	0	0	0	$-\frac{1}{48}$	$\frac{1}{24}$	0	$-\frac{1}{48}$	$\frac{1}{16}$	0	0	0

References

- [1] **Particle Data Group** Collaboration, R. L. Workman *et al.*, “Review of Particle Physics,” *PTEP* **2022** (2022) 083C01.
- [2] **Belle** Collaboration, S. K. Choi *et al.*, “Observation of a narrow charmonium-like state in exclusive $B^\pm \rightarrow K^\pm \pi^+ \pi^- J/\psi$ decays,” *Phys. Rev. Lett.* **91** (2003) 262001, [arXiv:hep-ex/0309032](#).
- [3] **BaBar** Collaboration, B. Aubert *et al.*, “Observation of a narrow meson decaying to $D_s^+ \pi^0$ at a mass of 2.32 GeV/ c^2 ,” *Phys. Rev. Lett.* **90** (2003) 242001, [arXiv:hep-ex/0304021](#).
- [4] **Belle** Collaboration, P. Krokovny *et al.*, “Observation of the $D_{sJ}(2317)$ and $D_{sJ}(2457)$ in B decays,” *Phys. Rev. Lett.* **91** (2003) 262002, [arXiv:hep-ex/0308019](#).
- [5] **CLEO** Collaboration, D. Besson *et al.*, “Observation of a narrow resonance of mass 2.46 GeV/ c^2 decaying to $D_s^{*+} \pi^0$ and confirmation of the $D_{sJ}^*(2317)$ state,” *Phys. Rev. D* **68** (2003) 032002, [arXiv:hep-ex/0305100](#). [Erratum: *Phys.Rev.D* 75, 119908 (2007)].
- [6] H.-X. Chen, W. Chen, X. Liu, and S.-L. Zhu, “The hidden-charm pentaquark and tetraquark states,” *Phys. Rept.* **639** (2016) 1–121, [arXiv:1601.02092 \[hep-ph\]](#).
- [7] F.-K. Guo, C. Hanhart, U.-G. Meißner, Q. Wang, Q. Zhao, and B.-S. Zou, “Hadronic molecules,” *Rev. Mod. Phys.* **90** no. 1, (2018) 015004, [arXiv:1705.00141 \[hep-ph\]](#). [Erratum: *Rev.Mod.Phys.* 94, 029901 (2022)].
- [8] Y.-R. Liu, H.-X. Chen, W. Chen, X. Liu, and S.-L. Zhu, “Pentaquark and Tetraquark states,” *Prog. Part. Nucl. Phys.* **107** (2019) 237–320, [arXiv:1903.11976 \[hep-ph\]](#).
- [9] R. F. Lebed, R. E. Mitchell, and E. S. Swanson, “Heavy-Quark QCD Exotica,” *Prog. Part. Nucl. Phys.* **93** (2017) 143–194, [arXiv:1610.04528 \[hep-ph\]](#).
- [10] A. Esposito, A. Pilloni, and A. D. Polosa, “Multiquark Resonances,” *Phys. Rept.* **668** (2017) 1–97, [arXiv:1611.07920 \[hep-ph\]](#).
- [11] N. Brambilla, S. Eidelman, C. Hanhart, A. Nefediev, C.-P. Shen, C. E. Thomas, A. Vairo, and C.-Z. Yuan, “The XYZ states: experimental and theoretical status and perspectives,” *Phys. Rept.* **873** (2020) 1–154, [arXiv:1907.07583 \[hep-ex\]](#).
- [12] L. Meng, B. Wang, G.-J. Wang, and S.-L. Zhu, “Chiral perturbation theory for heavy hadrons and chiral effective field theory for heavy hadronic molecules,” *Phys. Rept.* **1019** (2023) 1–149, [arXiv:2204.08716 \[hep-ph\]](#).
- [13] **BaBar** Collaboration, B. Aubert *et al.*, “Observation of a charmed baryon decaying to $D^0 p$ at a mass near 2.94 GeV/ c^2 ,” *Phys. Rev. Lett.* **98** (2007) 012001, [arXiv:hep-ex/0603052](#).
- [14] **Belle** Collaboration, K. Abe *et al.*, “Experimental constraints on the Spin and Parity of the $\Lambda_c(2880)^+$,” *Phys. Rev. Lett.* **98** (2007) 262001, [arXiv:hep-ex/0608043](#).
- [15] **LHCb** Collaboration, R. Aaij *et al.*, “Study of the $D^0 p$ amplitude in $\Lambda_b^0 \rightarrow D^0 p \pi^-$ decays,” *JHEP* **05** (2017) 030, [arXiv:1701.07873 \[hep-ex\]](#).
- [16] S. Capstick and N. Isgur, “Baryons in a relativized quark model with chromodynamics,” *Phys. Rev. D* **34** no. 9, (1986) 2809–2835.
- [17] D. Ebert, R. N. Faustov, and V. O. Galkin, “Spectroscopy and Regge trajectories of heavy baryons in the relativistic quark-diquark picture,” *Phys. Rev. D* **84** (2011) 014025, [arXiv:1105.0583 \[hep-ph\]](#).
- [18] B. Chen, K.-W. Wei, and A. Zhang, “Assignments of Λ_Q and Ξ_Q baryons in the heavy quark-light diquark picture,” *Eur. Phys. J. A* **51** (2015) 82, [arXiv:1406.6561 \[hep-ph\]](#).
- [19] Q.-F. Lü, Y. Dong, X. Liu, and T. Matsuki, “Puzzle of the Λ_c Spectrum,” *Nucl. Phys. Rev.* **35** no. 1, (2018) 1–4, [arXiv:1610.09605 \[hep-ph\]](#).
- [20] X.-G. He, X.-Q. Li, X. Liu, and X.-Q. Zeng, “ $\Lambda_c(2940)^+$: A Possible molecular state?,” *Eur. Phys. J. C* **51** (2007) 883–889, [arXiv:hep-ph/0606015](#).
- [21] J. He, Y.-T. Ye, Z.-F. Sun, and X. Liu, “The observed charmed hadron $\Lambda_c(2940)^+$ and the $D^* N$ interaction,” *Phys. Rev. D* **82** (2010) 114029, [arXiv:1008.1500 \[hep-ph\]](#).
- [22] P. G. Ortega, D. R. Entem, and F. Fernandez, “Quark model description of the $\Lambda_c(2940)^+$ as a molecular $D^* N$ state and the possible existence of the $\Lambda_b(6248)$,” *Phys. Lett. B* **718** (2013) 1381–1384, [arXiv:1210.2633 \[hep-ph\]](#).
- [23] Y. Dong, A. Faessler, T. Gutsche, and V. E. Lyubovitskij, “Strong two-body decays of the $\Lambda_c(2940)^+$ in a hadronic molecule picture,” *Phys. Rev. D* **81** (2010) 014006, [arXiv:0910.1204 \[hep-ph\]](#).

- [24] Y. Dong, A. Faessler, T. Gutsche, S. Kumano, and V. E. Lyubovitskij, “Radiative decay of $\Lambda_c(2940)^+$ in a hadronic molecule picture,” *Phys. Rev. D* **82** (2010) 034035, [arXiv:1006.4018 \[hep-ph\]](#).
- [25] J.-R. Zhang, “ S -wave $D^{(*)}N$ molecular states: $\Sigma_c(2800)$ and $\Lambda_c(2940)^{+?}$,” *Phys. Rev. D* **89** no. 9, (2014) 096006, [arXiv:1212.5325 \[hep-ph\]](#).
- [26] L. Zhao, H. Huang, and J. Ping, “ ND and NB systems in quark delocalization color screening model,” *Eur. Phys. J. A* **53** no. 2, (2017) 28, [arXiv:1612.00350 \[hep-ph\]](#).
- [27] E. Klempt and J.-M. Richard, “Baryon spectroscopy,” *Rev. Mod. Phys.* **82** (2010) 1095–1153, [arXiv:0901.2055 \[hep-ph\]](#).
- [28] V. Crede and W. Roberts, “Progress towards understanding baryon resonances,” *Rept. Prog. Phys.* **76** (2013) 076301, [arXiv:1302.7299 \[nucl-ex\]](#).
- [29] H.-Y. Cheng, “Charmed baryons circa 2015,” *Front. Phys. (Beijing)* **10** no. 6, (2015) 101406.
- [30] H.-X. Chen, W. Chen, X. Liu, Y.-R. Liu, and S.-L. Zhu, “A review of the open charm and open bottom systems,” *Rept. Prog. Phys.* **80** no. 7, (2017) 076201, [arXiv:1609.08928 \[hep-ph\]](#).
- [31] Y. Kato and T. Iijima, “Open charm hadron spectroscopy at B-factories,” *Prog. Part. Nucl. Phys.* **105** (2019) 61–81, [arXiv:1810.03748 \[hep-ex\]](#).
- [32] Y. Huang, J. He, J.-J. Xie, and L.-S. Geng, “Production of the $\Lambda_c(2940)$ by kaon-induced reactions on a proton target,” *Phys. Rev. D* **99** no. 1, (2019) 014045, [arXiv:1610.06994 \[hep-ph\]](#).
- [33] X.-Y. Wang, A. Guskov, and X.-R. Chen, “ $\Lambda_c^*(2940)^+$ photoproduction off the neutron,” *Phys. Rev. D* **92** no. 9, (2015) 094032, [arXiv:1509.02602 \[hep-ph\]](#).
- [34] H.-Y. Cheng and C.-K. Chua, “Strong Decays of Charmed Baryons in Heavy Hadron Chiral Perturbation Theory: An Update,” *Phys. Rev. D* **92** no. 7, (2015) 074014, [arXiv:1508.05653 \[hep-ph\]](#).
- [35] J.-J. Xie, Y.-B. Dong, and X. Cao, “Role of the $\Lambda_c^+(2940)$ in the $\pi^- p \rightarrow D^- D^0 p$ reaction close to threshold,” *Phys. Rev. D* **92** no. 3, (2015) 034029, [arXiv:1506.01133 \[hep-ph\]](#).
- [36] O. Romanets, L. Tolos, C. Garcia-Recio, J. Nieves, L. L. Salcedo, and R. G. E. Timmermans, “Charmed and strange baryon resonances with heavy-quark spin symmetry,” *Phys. Rev. D* **85** (2012) 114032, [arXiv:1202.2239 \[hep-ph\]](#).
- [37] J. He, Z. Ouyang, X. Liu, and X.-Q. Li, “Production of charmed baryon $\Lambda_c(2940)^+$ at PANDA,” *Phys. Rev. D* **84** (2011) 114010, [arXiv:1109.5566 \[hep-ph\]](#).
- [38] H.-Y. Cheng and C.-K. Chua, “Strong Decays of Charmed Baryons in Heavy Hadron Chiral Perturbation Theory,” *Phys. Rev. D* **75** (2007) 014006, [arXiv:hep-ph/0610283](#).
- [39] C. Chen, X.-L. Chen, X. Liu, W.-Z. Deng, and S.-L. Zhu, “Strong decays of charmed baryons,” *Phys. Rev. D* **75** (2007) 094017, [arXiv:0704.0075 \[hep-ph\]](#).
- [40] X.-H. Zhong and Q. Zhao, “Charmed baryon strong decays in a chiral quark model,” *Phys. Rev. D* **77** (2008) 074008, [arXiv:0711.4645 \[hep-ph\]](#).
- [41] H.-X. Chen, W. Chen, Q. Mao, A. Hosaka, X. Liu, and S.-L. Zhu, “P-wave charmed baryons from QCD sum rules,” *Phys. Rev. D* **91** no. 5, (2015) 054034, [arXiv:1502.01103 \[hep-ph\]](#).
- [42] S.-Q. Luo, B. Chen, Z.-W. Liu, and X. Liu, “Resolving the low mass puzzle of $\Lambda_c(2940)^+$,” *Eur. Phys. J. C* **80** no. 4, (2020) 301, [arXiv:1910.14545 \[hep-ph\]](#).
- [43] Y. Yan, X. Hu, Y. Wu, H. Huang, J. Ping, and Y. Yang, “Pentaquark interpretation of Λ_c states in the quark model,” *Eur. Phys. J. C* **83** no. 6, (2023) 524, [arXiv:2211.12129 \[hep-ph\]](#).
- [44] S.-Q. Luo, L.-S. Geng, and X. Liu, “Double-charm heptaquark states composed of two charmed mesons and one nucleon,” *Phys. Rev. D* **106** no. 1, (2022) 014017, [arXiv:2206.04586 \[hep-ph\]](#).
- [45] Z.-L. Zhang, Z.-W. Liu, S.-Q. Luo, F.-L. Wang, B. Wang, and H. Xu, “ $\Lambda_c(2910)$ and $\Lambda_c(2940)$ as conventional baryons dressed with the D^*N channel,” *Phys. Rev. D* **107** no. 3, (2023) 034036, [arXiv:2210.17188 \[hep-ph\]](#).
- [46] M.-J. Yan, F.-Z. Peng, and M. Pavon Valderrama, “Molecular charmed baryons and pentaquarks from light-meson exchange saturation,” *Phys. Rev. D* **109** no. 1, (2024) 014023, [arXiv:2304.14855 \[hep-ph\]](#).
- [47] Q. Xin, X.-S. Yang, and Z.-G. Wang, “The singly charmed pentaquark molecular states via the QCD sum rules,” *Int. J. Mod. Phys. A* **38** no. 22n23, (2023) 2350123, [arXiv:2307.08926 \[hep-ph\]](#).

- [48] U. Ozdem, “Electromagnetic properties of the $\Sigma_c(2800)^+$ and $\Lambda_c(2940)^+$ states via light-cone QCD,” *Eur. Phys. J. C* **83** no. 11, (2023) 1077, [arXiv:2309.00959 \[hep-ph\]](#).
- [49] H.-M. Yang and H.-X. Chen, “ $2P$ -wave charmed baryons from QCD sum rules,” [arXiv:2311.01991 \[hep-ph\]](#).
- [50] Belle Collaboration, R. Chistov *et al.*, “Observation of new states decaying into $\Lambda_c^+ K^- \pi^+$ and $\Lambda_c^+ K_S^0 \pi^-$,” *Phys. Rev. Lett.* **97** (2006) 162001, [arXiv:hep-ex/0606051](#).
- [51] BaBar Collaboration, B. Aubert *et al.*, “A Study of Excited Charm-Strange Baryons with Evidence for new Baryons $\Xi_c(3055)^+$ and $\Xi_c(3123)^+$,” *Phys. Rev. D* **77** (2008) 012002, [arXiv:0710.5763 \[hep-ex\]](#).
- [52] Belle Collaboration, Y. Kato *et al.*, “Search for doubly charmed baryons and study of charmed strange baryons at Belle,” *Phys. Rev. D* **89** no. 5, (2014) 052003, [arXiv:1312.1026 \[hep-ex\]](#).
- [53] Belle Collaboration, Y. Kato *et al.*, “Studies of charmed strange baryons in the ΛD final state at Belle,” *Phys. Rev. D* **94** no. 3, (2016) 032002, [arXiv:1605.09103 \[hep-ex\]](#).
- [54] X. Liu, C. Chen, W.-Z. Deng, and X.-L. Chen, “A Note on $\Xi_c(3055)^+$ and $\Xi_c(3123)^+$,” *Chin. Phys. C* **32** (2008) 424, [arXiv:0710.0187 \[hep-ph\]](#).
- [55] X.-H. Guo, K.-W. Wei, and X.-H. Wu, “Some mass relations for mesons and baryons in Regge phenomenology,” *Phys. Rev. D* **78** (2008) 056005, [arXiv:0809.1702 \[hep-ph\]](#).
- [56] L.-H. Liu, L.-Y. Xiao, and X.-H. Zhong, “Charm-strange baryon strong decays in a chiral quark model,” *Phys. Rev. D* **86** (2012) 034024, [arXiv:1205.2943 \[hep-ph\]](#).
- [57] Z. Zhao, D.-D. Ye, and A. Zhang, “Nature of charmed strange baryons $\Xi_c(3055)$ and $\Xi_c(3080)$,” *Phys. Rev. D* **94** no. 11, (2016) 114020, [arXiv:1608.04856 \[hep-ph\]](#).
- [58] H.-X. Chen, Q. Mao, A. Hosaka, X. Liu, and S.-L. Zhu, “D-wave charmed and bottomed baryons from QCD sum rules,” *Phys. Rev. D* **94** no. 11, (2016) 114016, [arXiv:1611.02677 \[hep-ph\]](#).
- [59] B. Chen, X. Liu, and A. Zhang, “Newly observed $\Lambda_c(2860)^+$ at LHCb and its D-wave partners $\Lambda_c(2880)^+$, $\Xi_c(3055)^+$ and $\Xi_c(3080)^+$,” *Phys. Rev. D* **95** no. 7, (2017) 074022, [arXiv:1702.04106 \[hep-ph\]](#).
- [60] Z.-G. Wang, “The $\Lambda_c(2860)$, $\Lambda_c(2880)$, $\Xi_c(3055)$ and $\Xi_c(3080)$ as D-wave baryon states in QCD,” *Nucl. Phys. B* **926** (2018) 467–490, [arXiv:1705.07745 \[hep-ph\]](#).
- [61] Y.-X. Yao, K.-L. Wang, and X.-H. Zhong, “Strong and radiative decays of the low-lying D-wave singly heavy baryons,” *Phys. Rev. D* **98** no. 7, (2018) 076015, [arXiv:1803.00364 \[hep-ph\]](#).
- [62] D.-D. Ye, Z. Zhao, and A. Zhang, “Study of P -wave excitations of observed charmed strange baryons,” *Phys. Rev. D* **96** no. 11, (2017) 114009, [arXiv:1709.00689 \[hep-ph\]](#).
- [63] D.-D. Ye, Z. Zhao, and A. Zhang, “Study of $2S$ - and $1D$ - excitations of observed charmed strange baryons,” *Phys. Rev. D* **96** no. 11, (2017) 114003, [arXiv:1710.10165 \[hep-ph\]](#).
- [64] Q. X. Yu, R. Pavao, V. R. Debastiani, and E. Oset, “Description of the Ξ_c and Ξ_b states as molecular states,” *Eur. Phys. J. C* **79** no. 2, (2019) 167, [arXiv:1811.11738 \[hep-ph\]](#).
- [65] K. Tsushima, D.-H. Lu, A. W. Thomas, K. Saito, and R. H. Landau, “Charmed mesic nuclei,” *Phys. Rev. C* **59** (1999) 2824–2828, [arXiv:nucl-th/9810016](#).
- [66] C. Garcia-Recio, J. Nieves, and L. Tolos, “D mesic nuclei,” *Phys. Lett. B* **690** (2010) 369–375, [arXiv:1004.2634 \[nucl-th\]](#).
- [67] A. Hosaka, T. Hyodo, K. Sudoh, Y. Yamaguchi, and S. Yasui, “Heavy Hadrons in Nuclear Matter,” *Prog. Part. Nucl. Phys.* **96** (2017) 88–153, [arXiv:1606.08685 \[hep-ph\]](#).
- [68] G. Krein, A. W. Thomas, and K. Tsushima, “Nuclear-bound quarkonia and heavy-flavor hadrons,” *Prog. Part. Nucl. Phys.* **100** (2018) 161–210, [arXiv:1706.02688 \[hep-ph\]](#).
- [69] R. Machleidt, K. Holinde, and C. Elster, “The Bonn Meson Exchange Model for the Nucleon Nucleon Interaction,” *Phys. Rept.* **149** (1987) 1–89.
- [70] J. Haidenbauer, G. Krein, U.-G. Meißner, and A. Sibirtsev, “Anti-D N interaction from meson-exchange and quark-gluon dynamics,” *Eur. Phys. J. A* **33** (2007) 107–117, [arXiv:0704.3668 \[nucl-th\]](#).
- [71] J. Haidenbauer, G. Krein, U.-G. Meißner, and A. Sibirtsev, “Charmed meson rescattering in the reaction $\bar{p}d \rightarrow \bar{D}DN$,” *Eur. Phys. J. A* **37** (2008) 55–67, [arXiv:0803.3752 \[hep-ph\]](#).
- [72] J. Haidenbauer, G. Krein, U.-G. Meißner, and L. Tolos, “DN interaction from meson exchange,” *Eur. Phys. J. A* **47** (2011) 18, [arXiv:1008.3794 \[nucl-th\]](#).
- [73] S. Weinberg, “Nuclear forces from chiral Lagrangians,” *Phys. Lett. B* **251** (1990) 288–292.

- [74] S. Weinberg, “Effective chiral Lagrangians for nucleon - pion interactions and nuclear forces,” *Nucl. Phys. B* **363** (1991) 3–18.
- [75] V. Bernard, N. Kaiser, and U.-G. Meißner, “Chiral dynamics in nucleons and nuclei,” *Int. J. Mod. Phys. E* **4** (1995) 193–346, [arXiv:hep-ph/9501384](#).
- [76] E. Epelbaum, H.-W. Hammer, and U.-G. Meißner, “Modern Theory of Nuclear Forces,” *Rev. Mod. Phys.* **81** (2009) 1773–1825, [arXiv:0811.1338 \[nucl-th\]](#).
- [77] R. Machleidt and D. R. Entem, “Chiral effective field theory and nuclear forces,” *Phys. Rept.* **503** (2011) 1–75, [arXiv:1105.2919 \[nucl-th\]](#).
- [78] U.-G. Meißner, “The long and winding road from chiral effective Lagrangians to nuclear structure,” *Phys. Scripta* **91** no. 3, (2016) 033005, [arXiv:1510.03230 \[nucl-th\]](#).
- [79] H. W. Hammer, S. König, and U. van Kolck, “Nuclear effective field theory: status and perspectives,” *Rev. Mod. Phys.* **92** no. 2, (2020) 025004, [arXiv:1906.12122 \[nucl-th\]](#).
- [80] F. Machleidt and F. Sammarruca, “Can chiral EFT give us satisfaction?,” *Eur. Phys. J. A* **56** no. 3, (2020) 95, [arXiv:2001.05615 \[nucl-th\]](#).
- [81] Z.-W. Liu, N. Li, and S.-L. Zhu, “Chiral perturbation theory and the $\bar{B}\bar{B}$ strong interaction,” *Phys. Rev. D* **89** no. 7, (2014) 074015, [arXiv:1211.3578 \[hep-ph\]](#).
- [82] H. Xu, B. Wang, Z.-W. Liu, and X. Liu, “ DD^* potentials in chiral perturbation theory and possible molecular states,” *Phys. Rev. D* **99** no. 1, (2019) 014027, [arXiv:1708.06918 \[hep-ph\]](#). [Erratum: Phys.Rev.D 104, 119903 (2021)].
- [83] B. Wang, Z.-W. Liu, and X. Liu, “ $\bar{B}^{(*)}\bar{B}^{(*)}$ interactions in chiral effective field theory,” *Phys. Rev. D* **99** no. 3, (2019) 036007, [arXiv:1812.04457 \[hep-ph\]](#).
- [84] L. Meng, B. Wang, G.-J. Wang, and S.-L. Zhu, “The hidden charm pentaquark states and $\Sigma_c\bar{D}^{(*)}$ interaction in chiral perturbation theory,” *Phys. Rev. D* **100** no. 1, (2019) 014031, [arXiv:1905.04113 \[hep-ph\]](#).
- [85] B. Wang, L. Meng, and S.-L. Zhu, “Hidden-charm and hidden-bottom molecular pentaquarks in chiral effective field theory,” *JHEP* **11** (2019) 108, [arXiv:1909.13054 \[hep-ph\]](#).
- [86] L. Meng, B. Wang, and S.-L. Zhu, “ $\Sigma_c N$ interaction in chiral effective field theory,” *Phys. Rev. C* **101** no. 6, (2020) 064002, [arXiv:1912.09661 \[nucl-th\]](#).
- [87] B. Wang, L. Meng, and S.-L. Zhu, “Spectrum of the strange hidden charm molecular pentaquarks in chiral effective field theory,” *Phys. Rev. D* **101** no. 3, (2020) 034018, [arXiv:1912.12592 \[hep-ph\]](#).
- [88] B. Wang, L. Meng, and S.-L. Zhu, “Deciphering the charged heavy quarkoniumlike states in chiral effective field theory,” *Phys. Rev. D* **102** (2020) 114019, [arXiv:2009.01980 \[hep-ph\]](#).
- [89] J.-B. Cheng, B.-L. Huang, Z.-Y. Lin, and S.-L. Zhu, “ Z_{cs} , Z_c and Z_b states under the complex scaling method,” *Eur. Phys. J. C* **83** no. 11, (2023) 1071, [arXiv:2305.15787 \[hep-ph\]](#).
- [90] Z.-Y. Lin, J.-B. Cheng, B.-L. Huang, and S.-L. Zhu, “Partial widths from analytical extension of the wave function: P_c states,” *Phys. Rev. D* **108** no. 11, (2023) 114014, [arXiv:2305.19073 \[hep-ph\]](#).
- [91] B. Wang, L. Meng, and S.-L. Zhu, “ $D^{(*)}N$ interaction and the structure of $\Sigma_c(2800)$ and $\Lambda_c(2940)$ in chiral effective field theory,” *Phys. Rev. D* **101** no. 9, (2020) 094035, [arXiv:2003.05688 \[hep-ph\]](#).
- [92] N. Kaiser, “Chiral corrections to kaon nucleon scattering lengths,” *Phys. Rev. C* **64** (2001) 045204, [arXiv:nucl-th/0107006](#). [Erratum: Phys.Rev.C 73, 069902 (2006)].
- [93] Y.-R. Liu and S.-L. Zhu, “Meson-baryon scattering lengths in heavy baryon chiral perturbation theory,” *Phys. Rev. D* **75** (2007) 034003, [arXiv:hep-ph/0607100](#).
- [94] B.-L. Huang and Y.-D. Li, “Kaon-nucleon scattering to one-loop order in heavy baryon chiral perturbation theory,” *Phys. Rev. D* **92** no. 11, (2015) 114033, [arXiv:1612.06163 \[nucl-th\]](#). [Erratum: Phys.Rev.D 95, 019903 (2017)].
- [95] B.-L. Huang, J.-S. Zhang, Y.-D. Li, and N. Kaiser, “Meson-baryon scattering to one-loop order in heavy baryon chiral perturbation theory,” *Phys. Rev. D* **96** no. 1, (2017) 016021, [arXiv:1701.06018 \[nucl-th\]](#).
- [96] B.-L. Huang and J. Ou-Yang, “Pion-nucleon scattering to $\mathcal{O}(p^3)$ in heavy baryon SU(3)-flavor chiral perturbation theory,” *Phys. Rev. D* **101** no. 5, (2020) 056021, [arXiv:1911.00846 \[nucl-th\]](#).
- [97] B.-L. Huang, “Pion-nucleon scattering to order p^4 in SU(3) heavy baryon chiral

- perturbation theory,” *Phys. Rev. D* **102** no. 11, (2020) 116001, [arXiv:2007.01173 \[nucl-th\]](#).
- [98] B.-L. Huang, J.-B. Cheng, and S.-L. Zhu, “Peripheral nucleon-nucleon scattering at next-to-next-to-leading order in SU(3) heavy baryon chiral perturbation theory,” *Phys. Rev. D* **104** no. 11, (2021) 116030, [arXiv:2109.11348 \[nucl-th\]](#).
- [99] B.-L. Huang, Z.-Y. Lin, and S.-L. Zhu, “Light pseudoscalar meson and heavy meson scattering lengths to $\mathcal{O}(p^4)$ in heavy meson chiral perturbation theory,” *Phys. Rev. D* **105** no. 3, (2022) 036016, [arXiv:2112.13702 \[hep-ph\]](#).
- [100] J.-X. Lu, C.-X. Wang, Y. Xiao, L.-S. Geng, J. Meng, and P. Ring, “Accurate Relativistic Chiral Nucleon-Nucleon Interaction up to Next-to-Next-to-Leading Order,” *Phys. Rev. Lett.* **128** no. 14, (2022) 142002, [arXiv:2111.07766 \[nucl-th\]](#).
- [101] J.-X. Lu, L.-S. Geng, M. Doering, and M. Mai, “Cross-Channel Constraints on Resonant Antikaon-Nucleon Scattering,” *Phys. Rev. Lett.* **130** no. 7, (2023) 071902, [arXiv:2209.02471 \[hep-ph\]](#).
- [102] B.-L. Huang, Z.-Y. Lin, K. Chen, and S.-L. Zhu, “Phase shifts of the light pseudoscalar meson and heavy meson scattering in heavy meson chiral perturbation theory,” *Eur. Phys. J. C* **83** no. 1, (2023) 76, [arXiv:2205.02619 \[hep-ph\]](#).
- [103] B. Borasoy and U.-G. Meißner, “Chiral Expansion of Baryon Masses and σ -Terms,” *Annals Phys.* **254** (1997) 192–232, [arXiv:hep-ph/9607432](#).
- [104] B. Borasoy, “Baryon axial currents,” *Phys. Rev. D* **59** (1999) 054021, [arXiv:hep-ph/9811411](#).
- [105] R. F. Lebed, “Baryon decuplet mass relations in chiral perturbation theory,” *Nucl. Phys. B* **430** (1994) 295–318, [arXiv:hep-ph/9311234](#).
- [106] M. B. Wise, “Chiral perturbation theory for hadrons containing a heavy quark,” *Phys. Rev. D* **45** no. 7, (1992) R2188.
- [107] A. V. Manohar and M. B. Wise, *Heavy quark physics*, vol. 10. Camb.Monogr.Part.Phys.Nucl.Phys.Cosmol., 2000.
- [108] E. Epelbaum, W. Gloeckle, and U.-G. Meißner, “Improving the convergence of the chiral expansion for nuclear forces. 2. Low phases and the deuteron,” *Eur. Phys. J. A* **19** (2004) 401–412, [arXiv:nucl-th/0308010](#).
- [109] E. Epelbaum, W. Gloeckle, and U.-G. Meißner, “The Two-nucleon system at next-to-next-to-next-to-leading order,” *Nucl. Phys. A* **747** (2005) 362–424, [arXiv:nucl-th/0405048](#).
- [110] X.-W. Kang, J. Haidenbauer, and U.-G. Meißner, “Antinucleon-nucleon interaction in chiral effective field theory,” *JHEP* **02** (2014) 113, [arXiv:1311.1658 \[hep-ph\]](#).
- [111] D. R. Entem and R. Machleidt, “Accurate charge dependent nucleon nucleon potential at fourth order of chiral perturbation theory,” *Phys. Rev. C* **68** (2003) 041001, [arXiv:nucl-th/0304018](#).
- [112] E. Epelbaum, H. Krebs, and U. G. Meißner, “Improved chiral nucleon-nucleon potential up to next-to-next-to-next-to-leading order,” *Eur. Phys. J. A* **51** no. 5, (2015) 53, [arXiv:1412.0142 \[nucl-th\]](#).
- [113] L.-Y. Dai, J. Haidenbauer, and U.-G. Meißner, “Antinucleon-nucleon interaction at next-to-next-to-next-to-leading order in chiral effective field theory,” *JHEP* **07** (2017) 078, [arXiv:1702.02065 \[nucl-th\]](#).
- [114] C. C. Chang *et al.*, “A per-cent-level determination of the nucleon axial coupling from quantum chromodynamics,” *Nature* **558** no. 7708, (2018) 91–94, [arXiv:1805.12130 \[hep-lat\]](#).
- [115] B. Märkisch *et al.*, “Measurement of the Weak Axial-Vector Coupling Constant in the Decay of Free Neutrons Using a Pulsed Cold Neutron Beam,” *Phys. Rev. Lett.* **122** no. 24, (2019) 242501, [arXiv:1812.04666 \[nucl-ex\]](#).
- [116] M. N. Butler, M. J. Savage, and R. P. Springer, “Strong and electromagnetic decays of the baryon decuplet,” *Nucl. Phys. B* **399** (1993) 69–88, [arXiv:hep-ph/9211247](#).
- [117] CLEO Collaboration, S. Ahmed *et al.*, “First measurement of $\Gamma(D^{*+})$,” *Phys. Rev. Lett.* **87** (2001) 251801, [arXiv:hep-ex/0108013](#).
- [118] C. Isola, M. Ladisa, G. Nardulli, and P. Santorelli, “Charming penguins contributions in $B \rightarrow K^*\pi, K(\rho, \omega, \phi)$ decays,” *Phys. Rev. D* **68** (2003) 114001, [arXiv:hep-ph/0307367](#).
- [119] B. Wang, K. Chen, L. Meng, and S.-L. Zhu, “Spectrum of the molecular pentaquarks,” [arXiv:2312.13591 \[hep-ph\]](#).
- [120] LHCb Collaboration, R. Aaij *et al.*, “Observation of five new narrow Ω_c^0 states decaying

- to $\Xi_c^+ K^-$,” *Phys. Rev. Lett.* **118** no. 18, (2017) 182001, [arXiv:1703.04639 \[hep-ex\]](#).
- [121] C. Wang, L.-L. Liu, X.-W. Kang, X.-H. Guo, and R.-W. Wang, “Possible open-charmed pentaquark molecule $\Omega_c(3188)$ - the $D\Xi$ bound state - in the Bethe-Salpeter formalism,” *Eur. Phys. J. C* **78** no. 5, (2018) 407, [arXiv:1710.10850 \[hep-ph\]](#).
- [122] B. Chen and X. Liu, “New Ω_c^0 baryons discovered by LHCb as the members of $1P$ and $2S$ states,” *Phys. Rev. D* **96** no. 9, (2017) 094015, [arXiv:1704.02583 \[hep-ph\]](#).